A High Precision Three Degrees of Freedom Friction Drive Stage

by

Woo Sok Chang

B.S., Electrical Engineering
Seoul National University, 1988

and

M.S., Electrical Engineering
Seoul National University, 1990

SUBMITTED TO THE DEPARTMENT OF MECHANICAL ENGINEERING IN PARTIAL FULLFILLMENT OF THE REQUIREMENTS FOR THE DEGREE OF

MASTER OF SCIENCE IN MECHANICAL ENGINEERING
AT THE
MASSACHUSETTS INSTITUTE OF TECHNOLOGY

JUNE 1999

© 1999 Massachusetts Institute of Technology
All rights reserved

Signature of Author .....
Department of Mechanical Engineering
May 24, 1999

Certified by .....
Kamal Youcef-Toumi
Professor of Mechanical Engineering
Thesis Supervisor

Accepted by .....
Ain A. Sonin
Chairman, Department Committee on Graduate Students

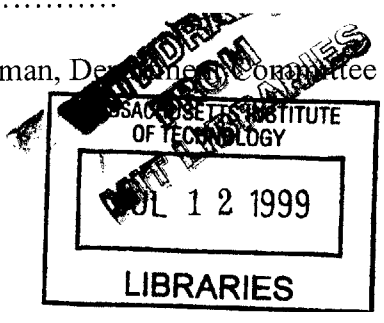

ENG

A High Precision Three Degrees of Freedom Friction Drive Stage

by

Woo Sok Chang

Submitted to the Department of Mechanical Engineering
on May 24, 1999 in Partial Fulfillment of the
Requirements of the Degree of Master of Science in
Mechanical Engineering

ABSTRACT

A friction drive high precision positioning stage is proposed in this thesis. The stage can move with three degrees of freedom, namely, two linear and one rotational motions. While conventional three degrees of freedom stage systems usually utilize three different one degree of freedom stages, the proposed system has only one movable stage for the three degrees of freedom. Therefore, this design has a simple structure and low cost. The stage uses three special actuation systems, each of which is designed so as to generate a directional elliptical motion, which allows the stage to move in a desired direction and/or rotation. In this thesis, the kinematic and dynamic models of the proposed system are presented, and the controllability and observability are shown. The bond graph modeling representation is used to offer a clear understanding of the general friction drive stage dynamic behavior. Simulation results demonstrate the feasibility of the design concept.

Thesis Supervisor: Kamal Youcef-Toumi

Title: Professor of Mechanical Engineering

Acknowledgement

I would like to thank the following people.

- Professor Kamal Youcef-Toumi for thesis guide and encouragement.
- Professor John Kassakian for giving me the time for writing this thesis.
- Dr. June Dong Kim and Dr. Sang-Gook Kim at Daewoo for support and encouragement.
- Professor Song-yop Hahn for teaching me how to do research.
- Professor Il Hong Suh for changing my life.
- Sangjoon Shin for having dinner with me lots of times for years.
- Jae-Hyuk Oh for assistance in the preparation of Section 3.6 and being a coffee partner.
- Labmates in Mechatronics Research Lab for useful discussion.
- KGSAME members for helping me to build a background in mechanical engineering.

Also, I would like to thank my wife, Eunchan, daughter, Yehna, son, Hweedo for their patience and understanding, my parents and Eunchan's parents for their prayer and encouragement.

Contents

List of Figures

1. Introduction

1.1. Motivation

The demand for high precision positioning stages has grown rapidly in some key industries. The applications include semiconductor manufacturing equipment, high precision machining optics (lenses and mirrors) and mass data storage. For example, semiconductor manufacturing equipment will soon require 0.1-1nm precision, and 30 cm x 30 cm travel range [Ohara96].

A friction drive system has a simple structure [Adachi]. Since no gear reduction unit is used in a friction drive system, no backlash exists. The position of the stage is very stable due to a large static frictional force. The friction drive system does not require a lubricant and therefore, it can be adequate for use in clean environments. Owing to the advantages mentioned above, a friction drive is considered as a candidate for high precision positioning stages. However, a friction drive requires strong wear resistant materials of which many reliable types have been reported [Ueha93]. Friction drive is appropriate for applications requiring small load but high precision since it is difficult to avoid slip in friction drive systems, and a driving force acting on a movable stage is usually limited by Coulomb friction force.

In practice, many 1 degree of freedom (DOF) or 2 DOF high precision friction drive stages have been developed. 1 DOF high precision friction drive positioning stages with nanometric

precision were reported [Ro94, Sakuta96]. Most of the developed high precision friction drive positioning stages are usually actuated with 2 DOF by the use of two 1 DOF stages [Burleigh, Mori89, Nikkei]. For 3 DOF motion such as X-Y-θ motion, the stage system usually uses three 1 DOF stages. Consequently, the system's structure and control scheme are more complex. In addition, the weight of the stage system itself is larger, and the cost of that is higher. On the other hand, some innovative 2 DOF friction driven stages, using only one stage, have been proposed by several researchers. However, most of the designs do not allow diagonal motion [Ferreira95, Choi96]. Each move is either in the X or Y direction at any one time, resulting in a slow rectangular motion. The reason for this is that the motion in one direction prevents the motion in the other direction. A 2 DOF stage design, which uses one stage and is capable of diagonal motion, was achieved by using a 2 DOF surface acoustic wave [Kurosawa96]. However, [Kurosawa96] reported that the stage is not reliable because it has aging problem due to very small vibration amplitude (5 nm), and the motion is unstable. This system may require expensive power electronic components due to its high operating frequency (10 MHz). [Hoshi95] proposed an array type of 2 DOF stage, which can move diagonally. In principle, this system can only move semi-diagonally because the number of movement direction choices is limited. Its cost may be high due to a complex structure.

1.2. Proposal of a high precision three degrees of freedom friction drive stage

In this thesis, a high precision friction drive positioning stage is proposed. The stage can move with 3 DOF, namely, two linear (X and Y) and one rotational (Θ about Z) motions. The proposed system has only one movable stage for 3 DOF. Therefore, this design has a simple

structure and low cost. The stage uses three special actuation systems, each of which is designed so as to generate a directional elliptical motion, which allows the stage to move in a desired direction and/or rotation.

1.3. Thesis outline

In this thesis, the kinematic and dynamic models of the proposed system are presented. The bond graph modeling representation is used to offer a clear understanding of the general friction drive stage dynamic behavior. In the following chapter, the operating principles of the proposed directional elliptical motion of an actuation system and the proposed 3 DOF friction drive stage using one movable stage and three actuation systems are presented. In Chapter 3, the proposed actuation system and the stage system are modeled and analyzed from kinematics and dynamics point of view. And the controllability and observability for the 3 DOF stage system are shown. Lastly, simulation results demonstrate the feasibility of the design concept in Chapter 4.

2. Operating principle of the proposed friction drive stage

2.1. Introduction

The operating principle of the proposed system is briefly presented in this chapter. For easy understanding, first, the operating principle of a 1 DOF friction drive stage using a conventional elliptical motion actuation system is explained. Secondly, the concept of the proposed directional elliptical motion is presented. Lastly, the operating principle of the proposed 3 DOF friction drive stage using three directional elliptical motion actuation systems is shown.

2.2. Operating principle of a 1 DOF friction drive stage using a conventional elliptical motion actuation system

For simplicity, we consider a conventional elliptical motion of an actuation system, shown in Figure 1. A 1 DOF stage, properly held by a bearing system, is free to move in the horizontal X direction. The stage is constrained by a preload force and its weight in the vertical Z direction. An actuation system generates X and Z vibration motions. The tip of the actuation system makes an elliptical locus such that the X and Z vibrations have the same frequency but with a 90 degree phase shift. The elliptical motion of the tip in the XZ plane allows the stage to move in the X direction by the friction force between the stage and the tip of the actuation system.

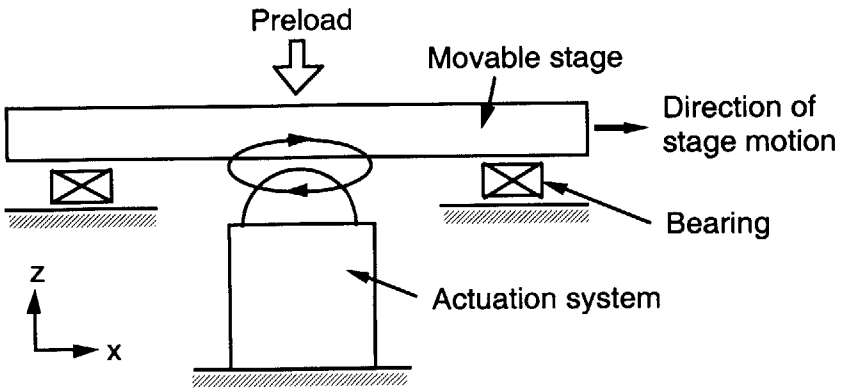

Figure 1: 1 DOF friction drive stage system including a conventional elliptical motion actuation system.

2.3. Operating principle of the proposed 3 DOF friction drive stage using three directional elliptical motion actuation systems

Now, instead of this actuation system for a 1 DOF motion of the stage, simply suppose another actuation system, which makes a directional elliptical locus motion as shown in Figure 2. This actuation system generates X, Y and Z vibration motions and the tip of the actuation system makes a directional elliptical locus by combining three vibrations appropriately. The tip is movable in a plurality of elliptical paths with each such path being in a plane orthogonal to the plane of the stage (i.e., the plane of the stage is the XY plane). A elliptical path can be disposed in the XZ plane and another elliptical path can be disposed in the YZ plane as well, more generally, the plane of the elliptical path of the tip can be rotatable through 360° about the Z axis.

The direction of the stage movement can be determined by the angle of the plane of the elliptical path of each actuation system and the amplitude of elliptical locus in practice. By controlling those parameters properly, the stage can move as desired. A 2 DOF linear motion of the stage in XY plane is shown in Figure 3. A rotational motion of the stage about Z is shown in Figure 4. In Figures 3 and 4, each of the loci corresponds to the motion of each of the three directional elliptical motion actuation systems. Here, by combining appropriately the linear and rotational motions, 3 DOF motion can be achieved.

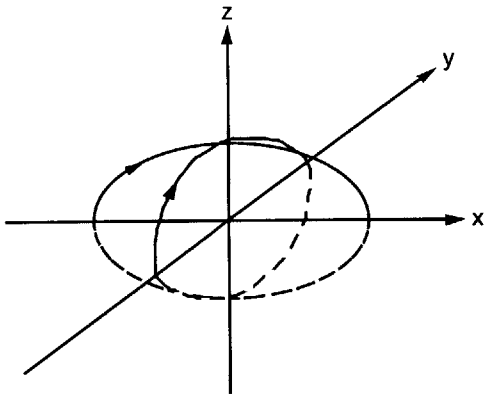

Figure 2: Directional elliptical motion of the tip of an actuation system (proposed).

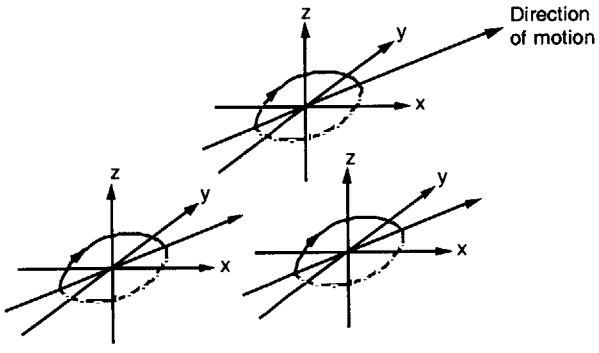

Figure 3: Exemplary elliptical loci of three actuation systems for moving a stage linearly in XY plane (proposed).

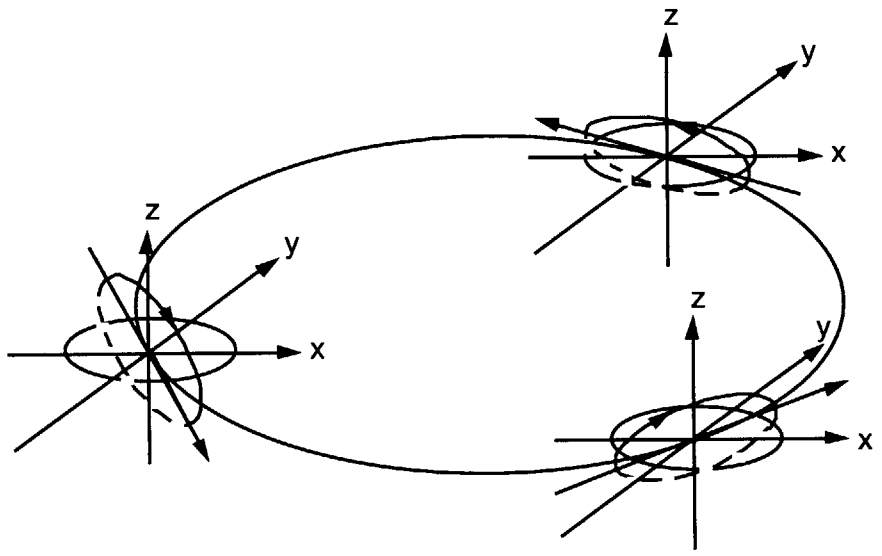

Figure 4: Exemplary elliptical loci of three actuation systems for rotating a stage (proposed).

2.4. Summary

The operating principle of the proposed 3 DOF friction drive stage was presented. The stage uses one movable stage and three special actuation systems, each of which is designed to generate a directional elliptical motion which allows the stage to move in X, Y and θ. Stated differently, the tip of each such actuation system is movable in an elliptical path disposed in a rotatable plane substantially orthogonal to the plane of the stage. Each of the actuation systems is independently controllable in order to permit the stage to be moved in 2-D (X and Y) as well as rotated (θ).

3. System modeling and analysis

3.1. Introduction

In this chapter, a directional elliptical motion actuation system is proposed. The kinematic analysis for the proposed actuation system is presented. For easy understanding of dynamics modeling of the proposed 3 DOF friction drive stage system, first, the modeling of a 2 DOF linear (XY) stage system with one directional elliptical motion actuation system is performed using Bond Graph. Next, based on the modeling of 2 DOF linear motion stage, the modeling of the proposed 3 DOF stage including one movable stage and three directional elliptical motion actuation systems is presented. Finally, the controllability and observability of the 3 DOF stage are presented.

3.2. An actuation system for directional elliptical motion

One possible actuation system, which generates a directional elliptical motion, is shown in Figure 5. Three piezoelectric elements are located and fixed on the circumference of a circle on an XY plane with radius r. The angle between the actuators elements is 120 degrees. Now, by appropriate combination of the three piezoelectric elements' elongation and constriction in the z direction, the end tip of the actuation system can be positioned in space with three degrees of freedom. For a directional motion of the actuation system, three degrees of freedom motion should be needed. Therefore, the desired direction elliptical motion can be achieved by this

design. The mathematical expression, relating the z directional motions of the three piezoelectric elements (z_1, z_2 and z_3) and the position vector of the tip (p_x, p_y and p_z), can be obtained using kinematic analysis. This is the topic of Section 3.3.

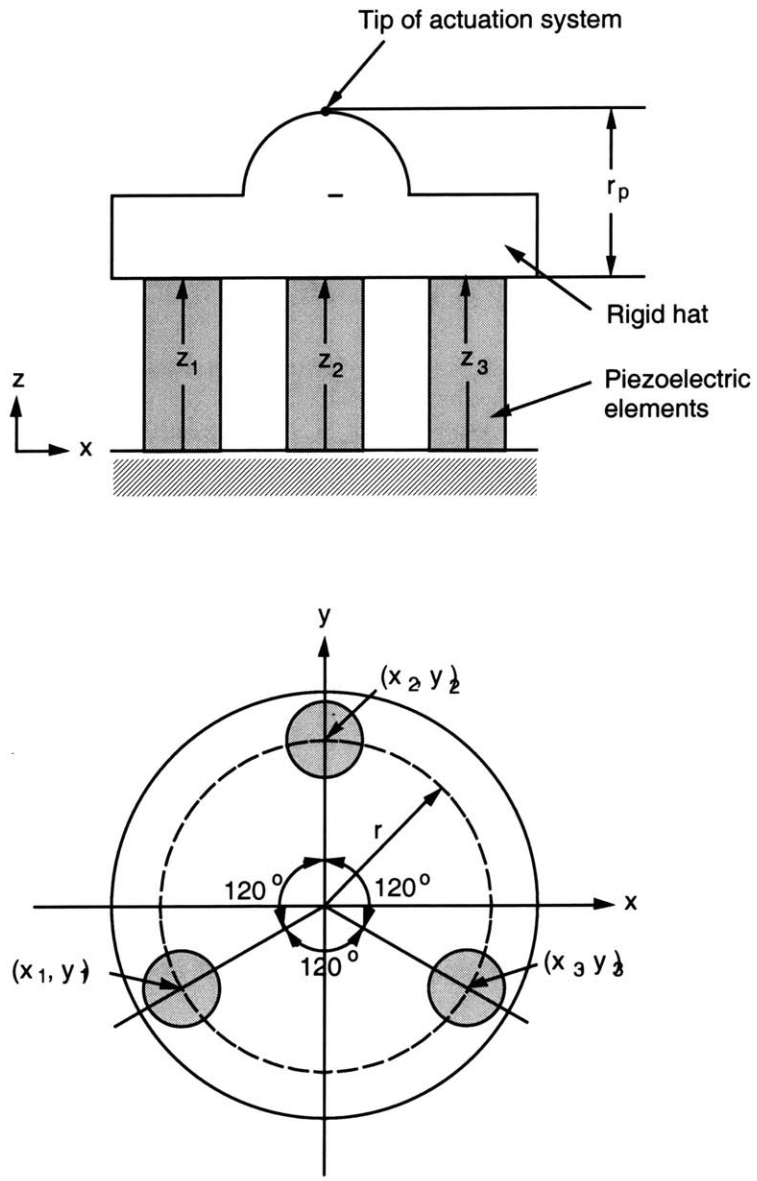

Figure 5: An actuation system capable of directional elliptical motion and its cross sectional view.

3.3. Kinematic analysis of the directional elliptical motion actuation system

The kinematics of the actuation system will be described using the following variables and parameters. The position of point **p**, located at the tip of the actuation system of Figure 5, and points $\mathbf{L}_1$, $\mathbf{L}_2$ and $\mathbf{L}_3$ are represented by the vectors $\mathbf{p}^T = [p_x, p_y, p_z]$, $\mathbf{L}_1{}^T = [x_1, y_1, z_1]$, $\mathbf{L}_2{}^T = [x_2, y_2, z_2]$, $\mathbf{L}_3{}^T = [x_3, y_3, z_3]$, respectively. The position of point **p** in terms of the elongation of the piezoelectric elements z_1, z_2 and z_3 are found to be,

$$\mathbf{p} = \begin{pmatrix} p_x \\ p_y \\ p_z \end{pmatrix} = \frac{\mathbf{L}_1 + \mathbf{L}_2 + \mathbf{L}_3}{3} + \frac{r_p}{\sqrt{a^2 + b^2 + 1}} \begin{pmatrix} a \\ b \\ 1 \end{pmatrix} \tag{1}$$

where r_p is given in Figure 5, and the constants a and b are given by

$$a = \frac{(-z_2 y_3 + z_3 y_2) - (-z_1 y_3 + z_3 y_1) + (-z_1 y_2 + z_2 y_1)}{(x_2 y_3 - x_3 y_2) - (x_1 y_3 - x_3 y_1) + (x_1 y_2 - x_2 y_1)}, \tag{2}$$

$$b = \frac{(-x_2 z_3 + x_3 z_2) - (-x_1 z_3 + x_3 z_1) + (-x_1 z_2 + x_2 z_1)}{(x_2 y_3 - x_3 y_2) - (x_1 y_3 - x_3 y_1) + (x_1 y_2 - x_2 y_1)}. \tag{3}$$

The component of the position vector of the tip, (p_x, p_y, p_z), is a nonlinear functions of z_1, z_2, and z_3. Here, let p_x be $f_1(z_1, z_2, z_3)$, p_y be $f_2(z_1, z_2, z_3)$, p_z be $f_3(z_1, z_2, z_3)$. Then, this expression can be used to determine relations for the velocities and forces as follows:

$$\begin{pmatrix} \delta p_x \\ \delta p_y \\ \delta p_z \end{pmatrix} = \mathbf{J}(z_1, z_2, z_3) \begin{pmatrix} \delta z_1 \\ \delta z_2 \\ \delta z_3 \end{pmatrix}, \tag{4}$$

where

$$J_{ij} = \left. \frac{\partial f_i}{\partial z_j} \right|_{(z_1, z_2, z_3)}. \tag{5}$$

Here, J_{ij} is an element of Jacobian matrix, and physically means the sensivity. For desired resolution of δp_i, δz_j is needed and determined by $\delta p_i / J_{ij}$. Therefore, the components of the position vector of the tip can be related to the elongation of three piezoelectric elements mathematically. Now differentiating with respect to time, the relation between the velocity vector of the tip and the z directional velocities of the three piezoelectric elements can be also obtained as,

$$\frac{d\mathbf{p}}{dt} = \mathbf{J}\left(\frac{dz_1}{dt}, \frac{dz_2}{dt}, \frac{dz_3}{dt} \right)^T. \tag{6}$$

Let the force of the tip and the force of three piezoelectric elements be represented by $\mathbf{f} = [f_x, f_y, f_z]^T$ and $\mathbf{F} = [F_1, F_2, F_3]^T$, respectively. Then the relation of these two forces are follows:

$$\mathbf{F} = \mathbf{J}^T \mathbf{f}. \tag{7}$$

3.4. Dynamic modeling of a 2 DOF stage with one directional elliptical motion actuation system

In order to understand the behavior of the proposed 3 DOF friction drive stage system, using the actuation system described in Section 3.2, in the first place, the dynamic analysis of a 2 DOF linear (XY) stage with one directional elliptical motion actuation system is carried out. In reality, this analysis is valid when the movable stage doesn't rotate during 2 DOF linear motion, for example, the center of mass of the circular planar movable stage moves along a line, which passes through the center of the stage. In fact, the analysis for a 2 DOF linear stage motion with one directional elliptical motion actuation system is fundamental for understanding the equations of motion for 3 DOF friction drive stage as in Figures 3 and 4. In other words, the equations of motion for the 3 DOF stage with three directional elliptical motion actuation systems are derived based on the dynamics modeling of a 2 DOF linear stage with one directional elliptical motion actuation system. The 2 DOF stage to be modeled is shown in Figure 6, and its associated bond graph model is depicted in Figure 7. In this model, the velocities in the x and y directions are outputs of the stage motion. Three voltages to three piezoelectric elements are inputs. Here, it is assumed that the stage is properly clamped and restrained to a fixed position in the z direction; but the z directional compliance of the friction material is considered. This means that the magnitude of the Coulomb friction force becomes a function of time. The driving forces for moving the stage in the x and y directions are dominantly composed of a Coulomb friction force and a viscous friction force. The compliance in the x and y directions is neglected. Also, the kinematic relation (Jacobian matrix) between the velocities and forces of the three piezoelectric elements and those of the tip are considered as in Section 3.3.

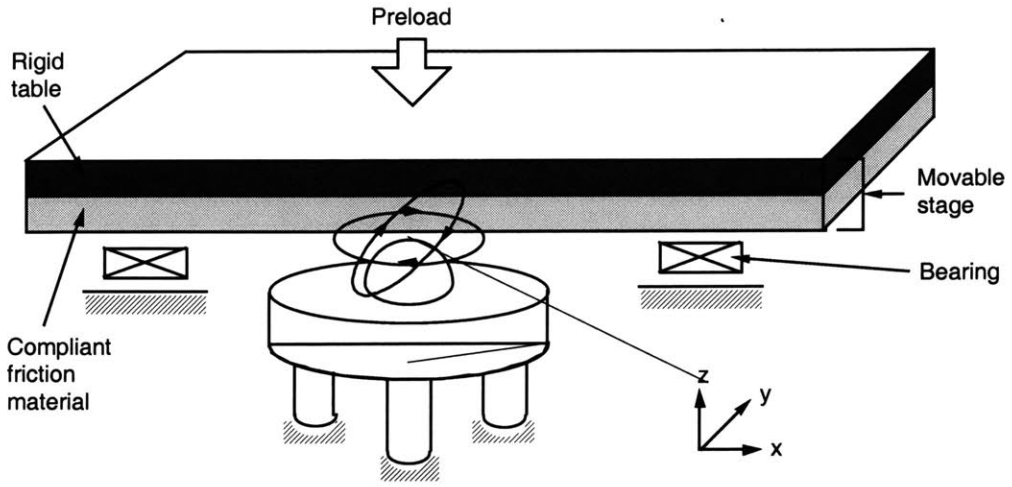

Figure 6: A 2 DOF friction drive stage including one directional elliptical motion actuation system.

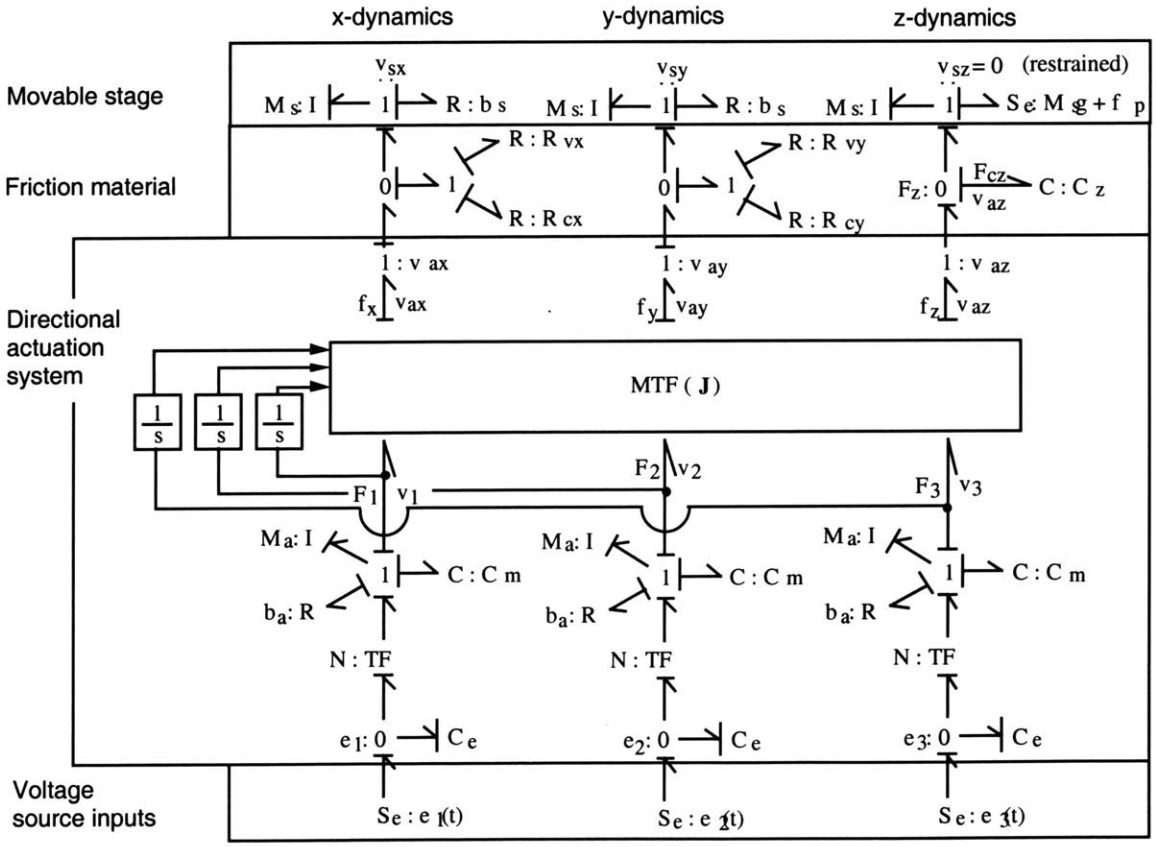

Figure 7: Bond graph model for the system of Figure 6.

Further assumptions include that the tip structure is rigid and its dynamics is neglected; and that the inputs to the piezoelectric elements are voltage sources. Note that when the tip does not contact the bottom surface of the stage, the power flow from the tip to the movable stage is zero. Therefore, load forces (F_1, F_2, F_3) from the actuation system side point of view are zeros, and effective driving forces acting on the movable stage (f_x, f_y, f_z) are zero, too.

In Figure 7, $e_1(t)$, $e_2(t)$, and $e_3(t)$ are voltage inputs to each piezoelectric element; C_e and C_m are electrical and mechanical capacitances of each piezoelectric element, respectively; TF is a transformer; N is the transformer modulus; M_a is the mass of each piezoelectric element; b_a is the mechanical resistance of each piezoelectric element; $v_1 = dz_1/dt$, $v_2 = dz_2/dt$, $v_3 = dz_3/dt$, are the z directional velocities of piezoelectric elements #1, #2 and #3 respectively; MTF is a modulated transformer (**J**); v_{ax}, v_{ay}, v_{az}: x, y, z velocities of the actuation system respectively; the variables f_x, f_y, f_z, F_1, F_2, F_3 were defined in Section 3.3; R_v ($=R_{vx}=R_{vy}$) and R_c ($=R_{cx}=R_{cy}$) are viscous and Coulomb friction resistances, respectively; M_s is the mass of the stage; b_s is the mechanical resistance of the stage; C_z ($1/k_z$) is the mechanical compliance (1/stiffness) of the friction material in the z direction; v_{sx}, v_{sy}, v_{sz} are the stage velocities in the x, y and z directions respectively; M_sg is the stage gravitation force; μ is a friction coefficient; and f_p is the preloaded force.

The causalities in the bond graph model of Figure 7 explain that the actuation system driven by three piezoelectric elements with voltage inputs is a kind of velocity source to the rest of the system including the friction material and the stage. Of course, this velocity source is not ideal

but depends on its dynamics as well as dynamic loads. The x and y directional driving force sources acting on the movable stage are determined by constitutive laws for the viscous forces associated with R_v as well as the Coulomb friction forces associated with R_c. In other words, the relative velocity between the stage and the tip in each direction is acting on R_v and R_c, the resultant forces are determined by constitutive laws for those elements (R_v, R_c). And these forces become effective forces acting on the movable stage. Note that since the magnitude of the Coulomb friction force depends on F_{cz}, it is also a time varying function. During the contact period, the actuation system is connected to the movable stage from a power flow point of view, and the stage is accelerated by translated power from the actuation system. However, during the non-contact period, the stage system is completely isolated from the actuation system, and it undergoes a deceleration process due to viscous friction in bearing systems. The state equations for the model in Figure 7 during the contact period are given as follows:

$$M_s \frac{dv_{sx}}{dt} = -b_s v_{sx} + f_x , \tag{8}$$

$$M_s \frac{dv_{sy}}{dt} = -b_s v_{sy} + f_y , \tag{9}$$

$$\frac{1}{k_z}\frac{dF_{cz}}{dt} = v_{az} , \tag{10}$$

$$M_a \frac{dv_1}{dt} = -F_{cm1} - b_a v_1 + Ne_1(t) - F_1 , \tag{11}$$

$$M_a \frac{dv_2}{dt} = -F_{cm2} - b_a v_2 + Ne_2(t) - F_2 , \tag{12}$$

$$M_a \frac{dv_3}{dt} = -F_{cm3} - b_a v_3 + Ne_3(t) - F_3 , \tag{13}$$

$$\frac{1}{k_m}\frac{dF_{cm1}}{dt} = v_1, \tag{14}$$

$$\frac{1}{k_m}\frac{dF_{cm2}}{dt} = v_2, \tag{15}$$

$$\frac{1}{k_m}\frac{dF_{cm3}}{dt} = v_3, \tag{16}$$

where

$$f_x = \mu\frac{(v_{ax1} - v_{sx1})F_{cz}}{\sqrt{(v_{ax} - v_{sx})^2 + (v_{ay} - v_{sy})^2}} + R_x(v_{ax} - v_{sx}), \tag{17}$$

$$f_y = \mu\frac{(v_{ay} - v_{sy})F_{cz}}{\sqrt{(v_{ax} - v_{sx})^2 + (v_{ay} - v_{sy})^2}} + R_y(v_{ay} - v_{sy}), \tag{18}$$

$$v_{ax} = J_{11}v_1 + J_{12}v_2 + J_{13}v_3, \tag{19}$$

$$v_{ay} = J_{21}v_1 + J_{22}v_2 + J_{23}v_3, \tag{20}$$

$$v_{az} = J_{31}v_1 + J_{32}v_2 + J_{33}v_3, \tag{21}$$

$$F_1 = J_{11}f_x + J_{21}f_y + J_{31}f_z, \tag{22}$$

$$F_2 = J_{12}f_x + J_{22}f_y + J_{32}f_z, \tag{23}$$

$$F_3 = J_{13}f_x + J_{23}f_y + J_{33}f_z. \tag{24}$$

During non-contact period, a power flow from actuation system to movable stage is disconnected, and F_1, F_2, F_3, and f_x, f_y, f_z are all zeros in the equations of motion above.

3.5. Dynamic modeling of a 3 DOF stage with three directional elliptical motion actuation systems

Based on the dynamics analysis of 2 DOF linear stage with one directional elliptical motion actuation system in Section 3.4, the equations of motion for the 3 DOF stage with three directional elliptical motion actuation systems are derived. 3 DOF includes two linear (XY) and one rotational (θ) motions. Schematic view of the proposed 3 DOF friction drive stage is shown in Figure 8. In Figure 8, XYO represents an inertial reference frame. $\mathbf{r}$ is a position vector $[x_s(t), y_s(t)]^T$ of the center of mass of movable stage with respect to the inertial frame. $\theta_s(t)$ represents the angle of the movable stage with respect to ground. $\mathbf{r}_1=[a_1, b_1]^T$, $\mathbf{r}_2=[a_2, b_2]^T$, $\mathbf{r}_3=[a_3, b_3]^T$ represent the constant position vectors of three actuation systems on XY plane. Each actuation system has three piezoelectric elements. $\mathbf{F}_1=[f_{x1}, f_{y1}]^T$, $\mathbf{F}_2=[f_{x2}, f_{y2}]^T$, $\mathbf{F}_3=[f_{x3}, f_{y3}]^T$ represent forces acting on the movable stage by actuation system #1, #2, and #3, respectively. Those forces are determined by the relative velocities and Coulomb and viscous friction forces. Note that the relative velocity for each actuation system is given by the difference between the velocity of the tip of the actuation system and the velocity of the stage at the position of the actuation system. And note that the direction of a friction force is the same as that of a relative velocity. Electrical voltages are applied to each piezoelectric element. Since each actuation system includes 3 piezoelectric elements as shown in Figure 8, 9 voltage inputs are needed. The equations of

motion during contact period for the whole system in Figure 8 with the 9 voltage inputs are as follows:

$$M_s \frac{dv_{sx}}{dt} = -b_s v_{sx} + f_{x1} + f_{x2} + f_{x3}, \tag{25}$$

$$M_s \frac{dv_{sy}}{dt} = -b_s v_{sy} + f_{y1} + f_{y2} + f_{y3}, \tag{26}$$

$$I \frac{dv_{s\theta}}{dt} = -b_\theta v_{s\theta} + T, \tag{27}$$

$$\frac{1}{k_z} \frac{dF_{cz1}}{dt} = v_{az1}, \tag{28}$$

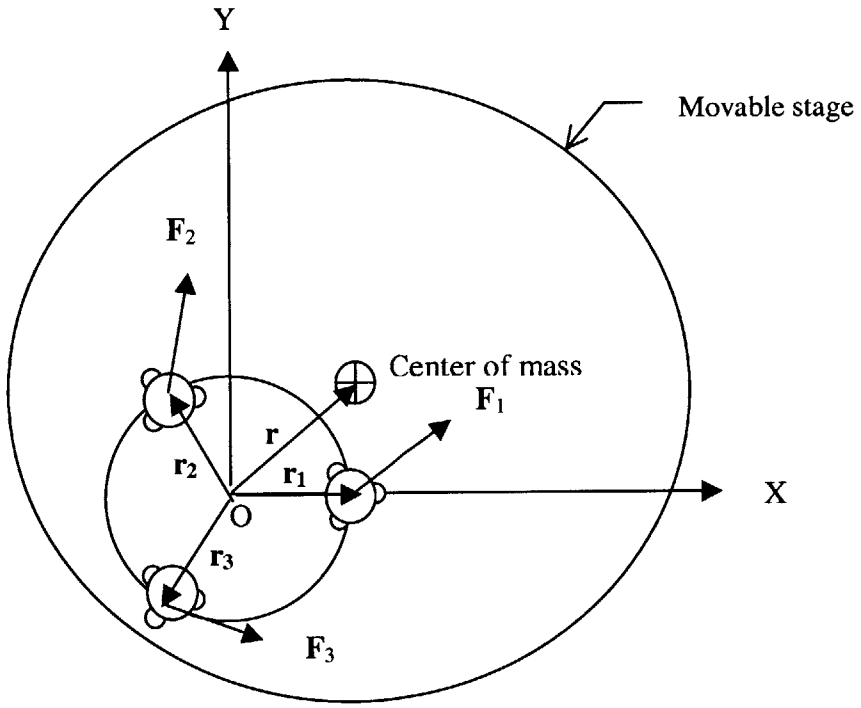

Figure 8: Schematic view of a 3 DOF friction drive stage.

$$\frac{1}{k_z}\frac{dF_{cz2}}{dt} = v_{az2}, \tag{29}$$

$$\frac{1}{k_z}\frac{dF_{cz3}}{dt} = v_{az3}, \tag{30}$$

$$M_a \frac{dv_{11}}{dt} = -F_{cm11} - b_a v_{11} + Ne_{11}(t) - F_{11}, \tag{31}$$

$$M_a \frac{dv_{21}}{dt} = -F_{cm21} - b_a v_{21} + Ne_{21}(t) - F_{21}, \tag{32}$$

$$M_a \frac{dv_{31}}{dt} = -F_{cm31} - b_a v_{31} + Ne_{31}(t) - F_{31}, \tag{33}$$

$$M_a \frac{dv_{12}}{dt} = -F_{cm12} - b_a v_{12} + Ne_{12}(t) - F_{12}, \tag{34}$$

$$M_a \frac{dv_{22}}{dt} = -F_{cm22} - b_a v_{22} + Ne_{22}(t) - F_{22}, \tag{35}$$

$$M_a \frac{dv_{32}}{dt} = -F_{cm32} - b_a v_{32} + Ne_{32}(t) - F_{32}, \tag{36}$$

$$M_a \frac{dv_{13}}{dt} = -F_{cm13} - b_a v_{13} + Ne_{13}(t) - F_{13}, \tag{37}$$

$$M_a \frac{dv_{23}}{dt} = -F_{cm23} - b_a v_{23} + Ne_{23}(t) - F_{23}, \tag{38}$$

$$M_a \frac{dv_{33}}{dt} = -F_{cm33} - b_a v_{33} + Ne_{33}(t) - F_{33}, \tag{39}$$

$$\frac{1}{k_m}\frac{dF_{cm11}}{dt} = v_{11}, \tag{40}$$

$$\frac{1}{k_m}\frac{dF_{cm21}}{dt} = v_{21}, \tag{41}$$

$$\frac{1}{k_m}\frac{dF_{cm31}}{dt} = v_{31}, \tag{42}$$

$$\frac{1}{k_m}\frac{dF_{cm12}}{dt} = v_{12}, \tag{43}$$

$$\frac{1}{k_m}\frac{dF_{cm22}}{dt} = v_{22}, \tag{44}$$

$$\frac{1}{k_m}\frac{dF_{cm32}}{dt} = v_{32}, \tag{45}$$

$$\frac{1}{k_m}\frac{dF_{cm13}}{dt} = v_{13}, \tag{46}$$

$$\frac{1}{k_m}\frac{dF_{cm23}}{dt} = v_{23}, \tag{47}$$

$$\frac{1}{k_m}\frac{dF_{cm33}}{dt} = v_{33}, \tag{48}$$

$$\frac{dx_s}{dt} = v_{sx}, \tag{49}$$

$$\frac{dy_s}{dt} = v_{sy}, \tag{50}$$

$$\frac{d\theta_s}{dt} = v_{s\theta}, \tag{51}$$

where

$$f_{x1} = \mu\frac{(v_{ax1} - v_{sx1})F_{cz1}}{\sqrt{(v_{ax1} - v_{sx1})^2 + (v_{ay1} - v_{sy1})^2}} + R_x(v_{ax1} - v_{sx1}), \tag{52}$$

$$f_{x2} = \mu \frac{(v_{ax2} - v_{sx2})F_{cz2}}{\sqrt{(v_{ax2} - v_{sx2})^2 + (v_{ay2} - v_{sy2})^2}} + R_x(v_{ax2} - v_{sx2}), \tag{53}$$

$$f_{x3} = \mu \frac{(v_{ax3} - v_{sx3})F_{cz3}}{\sqrt{(v_{ax3} - v_{sx3})^2 + (v_{ay3} - v_{sy3})^2}} + R_x(v_{ax3} - v_{sx3}), \tag{54}$$

$$f_{y1} = \mu \frac{(v_{ay1} - v_{sy1})F_{cz1}}{\sqrt{(v_{ax1} - v_{sx1})^2 + (v_{ay1} - v_{sy1})^2}} + R_y(v_{ay1} - v_{sy1}), \tag{55}$$

$$f_{y2} = \mu \frac{(v_{ay2} - v_{sy2})F_{cz2}}{\sqrt{(v_{ax2} - v_{sx2})^2 + (v_{ay2} - v_{sy2})^2}} + R_y(v_{ay2} - v_{sy2}), \tag{56}$$

$$f_{y3} = \mu \frac{(v_{ay3} - v_{sy3})F_{cz3}}{\sqrt{(v_{ax3} - v_{sx3})^2 + (v_{ay3} - v_{sy3})^2}} + R_y(v_{ay3} - v_{sy3}), \tag{57}$$

$$v_{sx1} = v_{sx} - b_1 v_{s\theta},\ v_{sx2} = v_{sx} - b_2 v_{s\theta},\ v_{sx3} = v_{sx} - b_3 v_{s\theta}, \tag{58}$$

$$v_{sy1} = v_{sy} + a_1 v_{s\theta},\ v_{sy2} = v_{sy} + a_2 v_{s\theta},\ v_{sy3} = v_{sy} + a_3 v_{s\theta}, \tag{59}$$

$$v_{ax1} = J_{11}v_{11} + J_{12}v_{21} + J_{13}v_{31},\ v_{ax2} = J_{11}v_{12} + J_{12}v_{22} + J_{13}v_{32},\ v_{ax3} = J_{11}v_{13} + J_{12}v_{23} + J_{13}v_{33}, \tag{60}$$

$$v_{ay1} = J_{21}v_{11} + J_{22}v_{21} + J_{23}v_{31},\ v_{ay2} = J_{21}v_{12} + J_{22}v_{22} + J_{23}v_{32},\ v_{ay3} = J_{21}v_{13} + J_{22}v_{23} + J_{23}v_{33}, \tag{61}$$

$$v_{az1} = J_{31}v_{11} + J_{32}v_{21} + J_{33}v_{31},\ v_{az2} = J_{31}v_{12} + J_{32}v_{22} + J_{33}v_{32},\ v_{az3} = J_{31}v_{13} + J_{32}v_{23} + J_{33}v_{33}, \tag{62}$$

$$F_{11} = J_{11}f_{x1} + J_{21}f_{y1} + J_{31}f_{z1},\ F_{21} = J_{12}f_{x1} + J_{22}f_{y1} + J_{32}f_{z1},\ F_{31} = J_{13}f_{x1} + J_{23}f_{y1} + J_{33}f_{z1}, \tag{63}$$

$$F_{12} = J_{11}f_{x2} + J_{21}f_{y2} + J_{31}f_{z2}, F_{22} = J_{12}f_{x2} + J_{22}f_{y2} + J_{32}f_{z2}, F_{32} = J_{13}f_{x2} + J_{23}f_{y2} + J_{33}f_{z2}, \tag{64}$$

$$F_{13} = J_{11}f_{x3} + J_{21}f_{y3} + J_{31}f_{z3}, F_{23} = J_{12}f_{x3} + J_{22}f_{y3} + J_{32}f_{z3}, F_{33} = J_{13}f_{x3} + J_{23}f_{y3} + J_{33}f_{z3}, \tag{65}$$

$$T = -x_s(f_{y1} + f_{y2} + f_{y3}) + y_s(f_{x1} + f_{x2} + f_{x3}) + (a_1 f_{y1} + a_2 f_{y2} + a_3 f_{y3}) - (b_1 f_{x1} + b_2 f_{x2} + b_3 f_{x3}) \quad (66)$$

In the equations of motion above, M_s is the mass of the stage; I represents the inertia of the stage; v_{sx}, v_{sy}, $v_{s\theta}$ are x, y component of stage velocity and angular velocity; b_s is viscous resistance of bearing; f_{xi}, f_{yi} are x, y components of the force by the i^{th} actuation system; **T** is the moment by three actuation systems; k_z is z directional stiffness of friction material; F_{czi} is z directional compliant force in friction material associated with the i^{th} actuation system; v_{azi} is z component of the actuator velocity associated with the i^{th} actuation system; M_a is actuator mass, v_{ij} is z component of the velocity of the i^{th} piezoelectric element of the j^{th} actuation system; F_{cmij} is mechanical compliant force in the i^{th} piezoelectric element of the j^{th} actuation system; e_{ij} represents the voltage input to the i^{th} piezoelectric element of the j^{th} actuation system; F_{ij}: z component of the force by the i^{th} piezoelectric element of the j^{th} actuation system; N is a transformer modulus in piezoelectric elements; k_m is mechanical stiffness in piezoelectric elements. x_s, y_s, θ_s: x, y, θ component of stage displacement; f_{xi}, f_{yi} in Equations (52-57) are x and y components of the force acting on the stage by the i^{th} actuation system, and those forces are composed of Coulomb and viscous friction forces. v_{sxi}, v_{syi} are x and y components of the stage velocity at the center of the i^{th} actuation system; (a_1, b_1), (a_2, b_2), and (a_3, b_3) are x and y positions of three actuation systems; v_{axi}, v_{ayi} are x and y components of the velocity of the tip of the i^{th} actuation system; J_{ij}: elements of Jacobian matrix. During non-contact period, power flow from actuation systems to the movable stage is disconnected as in Section 3.4, and F_{ij}, and f_{xi}, f_{yi}, f_{zi} are all zeros in the equations of motion above.

3.6. Controllability and observability

Reconsider the system shown in Figure 8. The variables for the system were defined in Section 3.5. For simplicity, assume that the sources by three actuation systems are ideal force sources. In practice, those force sources can be determined by both the amplitude of elliptical locus and the rotation angle of the plane of the elliptical locus for each actuation system. Now, the simplified equations of motion for the movable stage are as follows:

$$M_s \frac{d^2 x_s}{dt^2} + b_s \frac{dx_s}{dt} = f_{x1} + f_{x2} + f_{x3}, \tag{67}$$

$$M_s \frac{d^2 y_s}{dt^2} + b_s \frac{dy_s}{dt} = f_{y1} + f_{y2} + f_{y3}, \tag{68}$$

$$I \frac{d^2 \theta_s}{dt^2} + b_\theta \frac{d\theta_s}{dt} = T, \tag{69}$$

where

$$T = -x_s(f_{y1} + f_{y2} + f_{y3}) + y_s(f_{x1} + f_{x2} + f_{x3}) + (a_1 f_{y1} + a_2 f_{y2} + a_3 f_{y3}) - (b_1 f_{x1} + b_2 f_{x2} + b_3 f_{x3}) \tag{70}$$

Here, T is the z component of torque **T** of

$$\mathbf{T} = (\mathbf{r}_1 - \mathbf{r}) \times \mathbf{F}_1 + (\mathbf{r}_2 - \mathbf{r}) \times \mathbf{F}_2 + (\mathbf{r}_3 - \mathbf{r}) \times \mathbf{F}_3. \tag{71}$$

Let us define a new set of state variables,

$$\begin{pmatrix} x_1 \\ x_2 \\ x_3 \\ x_4 \\ x_5 \\ x_6 \end{pmatrix} = \begin{pmatrix} x_s \\ \dot{x}_s \\ y_s \\ \dot{y}_s \\ \theta_s \\ \dot{\theta}_s \end{pmatrix}.$$

Then, Equation (67-69) can be rewritten as a nonlinear state equation as follows:

$$d\mathbf{X}/dt = \mathbf{AX} + \mathbf{B}(\mathbf{X})\mathbf{u}, \tag{72}$$

where $\mathbf{X} = [x_1, x_2, x_3, x_4, x_5, x_6]^T$, $\mathbf{u} = [f_{x1}, f_{x2}, f_{x3}, f_{y1}, f_{y2}, f_{y3}]^T$,

$$\mathbf{A} = \begin{bmatrix} 0 & 1 & 0 & 0 & 0 & 0 \\ 0 & e1 & 0 & 0 & 0 & 0 \\ 0 & 0 & 0 & 1 & 0 & 0 \\ 0 & 0 & 0 & e2 & 0 & 0 \\ 0 & 0 & 0 & 0 & 0 & 1 \\ 0 & 0 & 0 & 0 & 0 & e3 \end{bmatrix}, \tag{73}$$

where $e1 = -b_x/M_s$, $e2 = -b_y/M_s$, $e3 = -b_\theta/I$,

$$\mathbf{B}=\begin{bmatrix} 0 & 0 & 0 & 0 & 0 & 0 \\ 1 & 1 & 1 & 0 & 0 & 0 \\ 0 & 0 & 0 & 0 & 0 & 0 \\ 0 & 0 & 0 & 1 & 1 & 1 \\ 0 & 0 & 0 & 0 & 0 & 0 \\ d1 & d2 & d3 & d4 & d5 & d6 \end{bmatrix}, \tag{74}$$

where $d1=-b_1+x_3$, $d2=-b_2+x_3$, $d3=-b_3+x_3$, $d4=a_1-x_1$, $d5=a_2-x_1$, $d6=a_3-x_1$.

Here, let us define a 3x6 matrix **E,** which is composed of nonzero rows of **B,**

$$\mathbf{E}=\begin{bmatrix} 1 & 1 & 1 & 0 & 0 & 0 \\ 0 & 0 & 0 & 1 & 1 & 1 \\ d1 & d2 & d3 & d4 & d5 & d6 \end{bmatrix}. \tag{75}$$

It is obvious that the rank of **E** is 3 unless d1=d2=d3 and d4=d5=d6. Note that d1=d2=d3 means that three actuation systems have the same Y locations, and d4=d5=d6 means that three actuation systems have the same X locations, physically. If the rank of **E** is 3, there exists a pseudo-inverse matrix of **E**, **G**, and the matrix **G** satisfies the following relation.

$$\mathbf{EG}=\mathbf{I}_3, \tag{76}$$

where $\mathbf{I}_3$ is 3x3 identity matrix. Here, note that **G** is not unique. Now, let us design a nonlinear feedback controller, **u** to linearize the system in Equation (72) as follows:

$$\mathbf{u}=\mathbf{Gv}, \tag{77}$$

where **v** is a new control input vector,

$$\mathbf{v} = [v_1, v_2, v_3]^T. \tag{78}$$

Then, the system can be linearized as follows:

$$d\mathbf{X}/dt = \mathbf{AX} + \mathbf{B(X)u} = \mathbf{AX} + \{\mathbf{B(X)\ G}\}\mathbf{v}, \tag{79}$$

where

$$\mathbf{BG} = \begin{bmatrix} 0 & 0 & 0 \\ 1 & 0 & 0 \\ 0 & 0 & 0 \\ 0 & 1 & 0 \\ 0 & 0 & 0 \\ 0 & 0 & 1 \end{bmatrix}.$$

From Equation (79), note that the three state variables, $x_s(t)$, $y_s(t)$, $\theta_s(t)$ are de-coupled. It is obvious that the controllability matrix for each sub state equation (i.e., subsystems for x_s, y_s, and θ_s) has a rank of two. And, the linearized system is controllable. In addition, since the observability matrix has a rank of two, the linearized system is observable as well for each de-coupled subsystem if the system output is position or velocity of the system. Now, consider a matrix **G**, which satisfies Equation (76). As mentioned previously, **G** is not unique. But here is one choice. $\mathbf{G} = \mathbf{E}^T(\mathbf{E}\mathbf{E}^T)^{-1}$. Then, $\mathbf{EG} = \mathbf{I}_3$. **G** always exists unless d1=d2=d3 and d4=d5=d6. Now, new control input to the system **u** can be rewritten as $\mathbf{u} = \mathbf{Gv}$. The controllability and

observability for the whole system with 9 voltages source instead of three force inputs can be studied in the future.

3.7. Summary

A special actuation system was proposed. The proposed actuation system was designed to generate directional elliptical motion. Using the concept of the directional elliptical actuation systems, a 3 DOF friction drive stage system was proposed and mathematically modeled. The proposed stage system uses one movable stage and three directional elliptical motion actuation systems. The controllability and observability for the system was presented.

4. 3 DOF motion simulation

4.1. Introduction

In order to verify the concept of the proposed stage in Equation (25-51), the 3 DOF stage motion is simulated. For easy understanding, first, a simple 2 DOF linear (XY) motion, secondly, a pure rotational motion, and finally, a general 3 DOF (linear plus rotational) motion are demonstrated. Common parameters for this simulation are as follows:

M_s: 1 [kg]; I: $5x10^{-3}$ [kg m^2]; M_a: 0.1 [kg]; C_m: $2x10^{-8}$ [m/N]; N: 8 [N/V]; g: 9.81 [m/sec2]; C_z: 10^{-7} [m/N]; b_s: 10^4 [kg/sec]; b_θ: 10^2 [Nsec/m]; b_a: 3 x 10^3 [kg/sec]; R_v: 10 [kg/sec]; μ: 0.2; r: 2 [cm]; r_p: 2 [cm]; $(x_1, y_1)=(r\cos(0), r\sin(0))$; $(x_2, y_2)=(r\cos(2\pi/3), r\sin(2\pi/3))$; $(x_3, y_3)=(r\cos(4\pi/3), r\sin(4\pi/3))$; gap distance between the tip and the bottom surface with zero voltages applied: 10^{-6} [m]; frequency of voltage input (f): 1 [kHz]; ratio of the horizontal amplitude to the vertical amplitude of an elliptical locus (a_r): 2. The voltage inputs (e_{ij}) to the i^{th} piezoelectric element of the j^{th} actuation system to generate a desired rotation angle of the elliptical locus plane, θ_j of the j^{th} actuation system are as follows:

$$e_{1j}(t) = 150\,\{\sin(2\pi f\,t) + a_r\cos(\theta_j)\cos(2\pi f\,t)\,(r/r_p)\}, \tag{80}$$

$$e_{2j}(t) = 150\,\{\sin(2\pi f\,t) - a_r\cos(\theta_j+\pi/3)\cos(2\pi f\,t)\,(r/r_p)\}, \tag{81}$$

$$e_{3j}(t) = 150\,\{\sin(2\pi f\,t) - a_r\cos(\theta_j-\pi/3)\cos(2\pi f\,t)\,(r/r_p)\}. \tag{82}$$

4.2. Simulation of a linear motion

In order to show a linear motion of the stage, θ_1, θ_2, θ_3 are all selected as 60° in this simulation as shown in Figure 9. The corresponding nine voltages in Equations (80-82) are applied to nine piezoelectric elements of three actuation systems. Time responses are obtained as the outputs of the simulation. Figures 10-12 show the time responses of the stage motion. The x, y, and θ displacements of the stage are represented by x_s, y_s, and θ_s. The X, Y components of velocity, and angular velocity about Z axis of the stage are represented by v_{sx}, v_{sy}, and $v_{s\theta}$. In each figure, to easily recognize the contact and non-contact periods, normal contact force, F_{cz} is also plotted. The time period of positive F_{cz} corresponds to the contact period. The larger the normal contact force is, the more the friction material is deformed. As expected, both x and y components of the velocity are increased during the contact period, and these are decreased during the non-contact period. Note that a high viscous friction resistance in the bearing system is used in this simulation for showing the motion of the stage dramatically. Due to the very high friction resistance of the bearings, the velocity of the stage is reduced to almost zero as expected during the non-contact period of every cycle. The time responses show that the velocity and displacement are consistent. In Figure 12, zero angle of rotation and zero angular velocity are shown as expected. In order to clearly confirm the direction of the simulated motion, the x-y plot is separately shown in Figure 13. The direction of the simulated stage motion is 60 degrees which is exactly the same as the input to the simulated model. For reference, Figures 14-16 show voltage inputs to each piezoelectric element of each actuation system. In these Figures, e_{ij} represents the voltage input to the i^{th} piezoelectric element of the j^{th} actuation system. Note that in this simulation, since $e_{1j}=e_{2j}$ for j=1, 2, 3, and those graphs are overlapped in Figures 14-16.

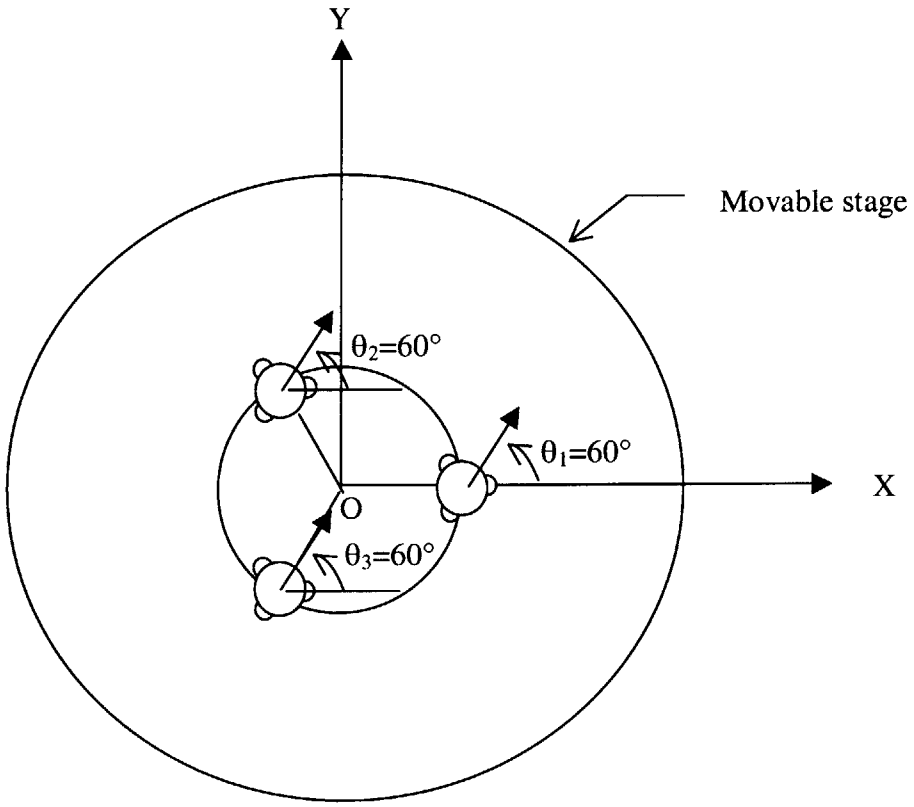

Figure 9: Schematic view of a 3 DOF friction drive stage moving linearly in XY plane.

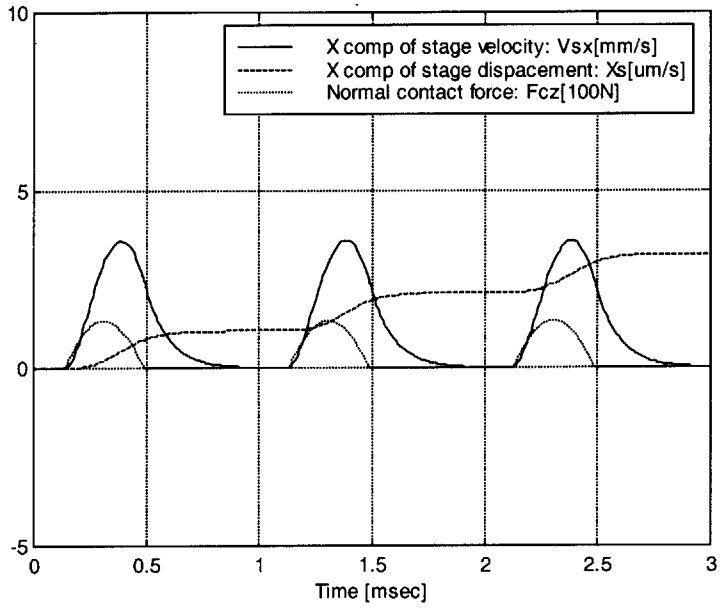

Figure 10: Time response of x component of stage velocity (v_{sx}) and displacement (x_s) to achieve a linear motion.

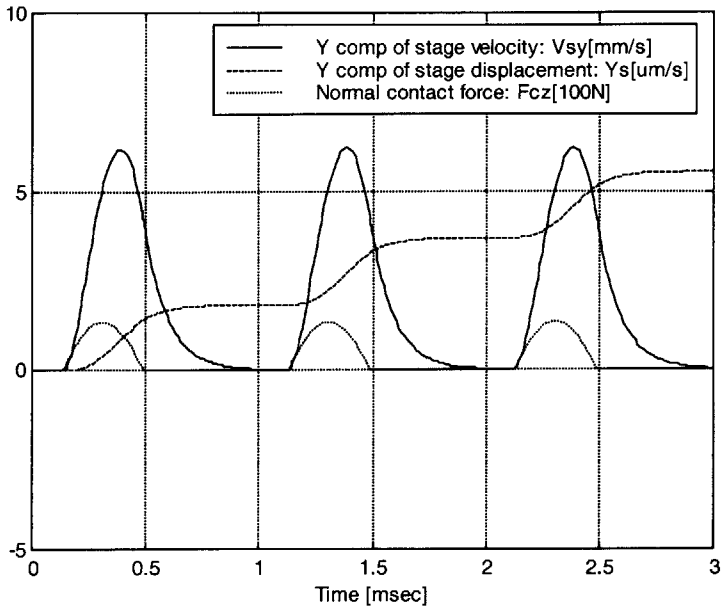

Figure 11: Time response of y component of stage velocity (v_{sy}) and displacement (y_s) to achieve a linear motion.

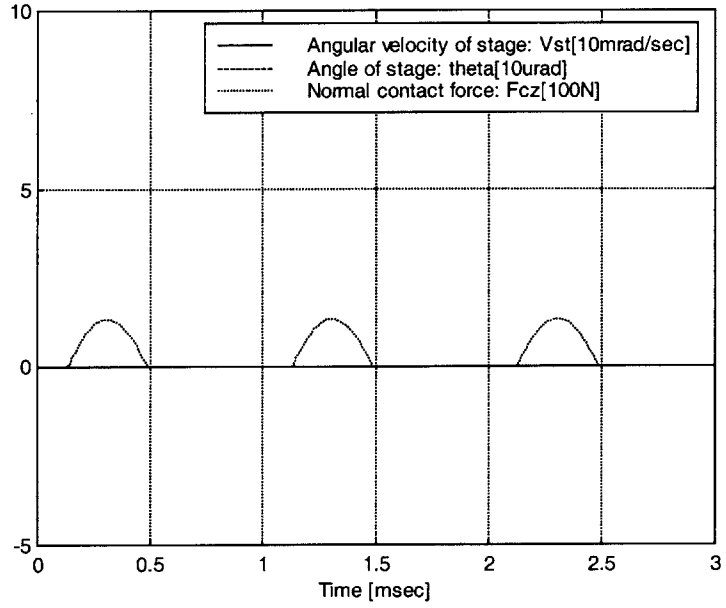

Figure 12: Time response of angular velocity ($v_{s\theta}$=Vst) and angle (θ=Theta) of the stage to achieve a linear motion.

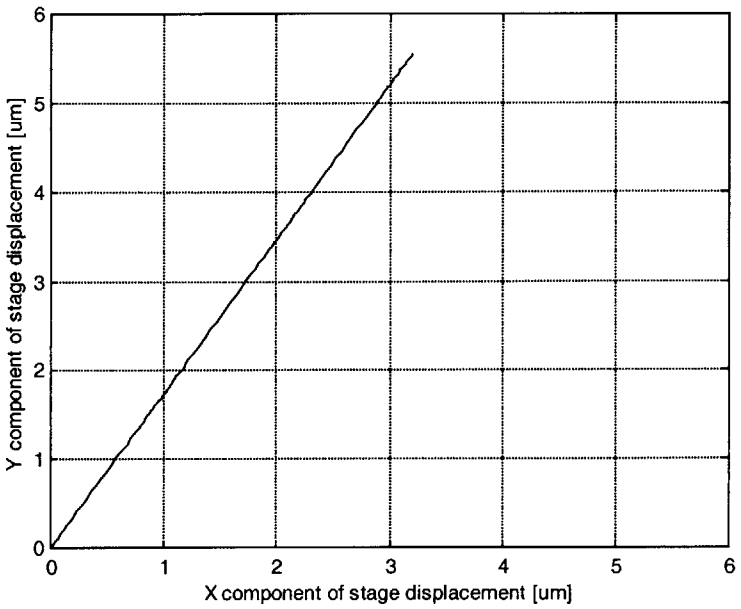

Figure 13: Trajectory of stage motion in XY plane to achieve a linear motion.

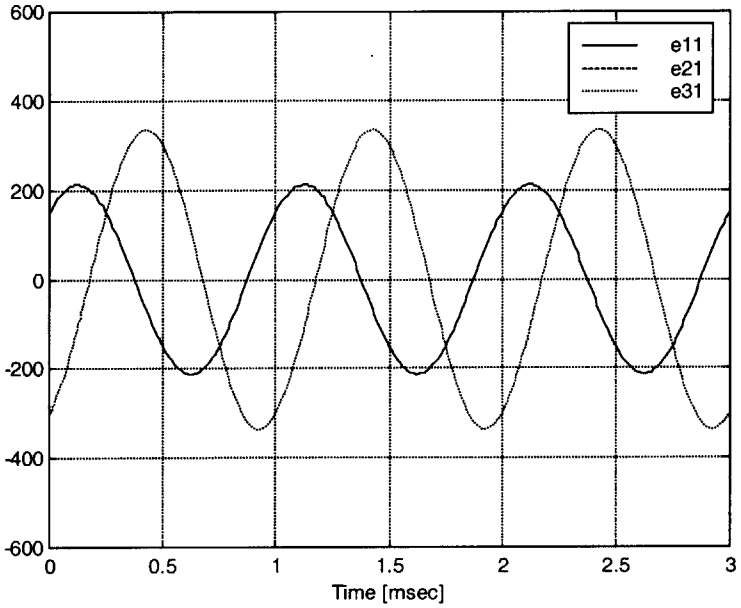

Figure 14: Voltage inputs for the first actuation system to achieve a linear motion.

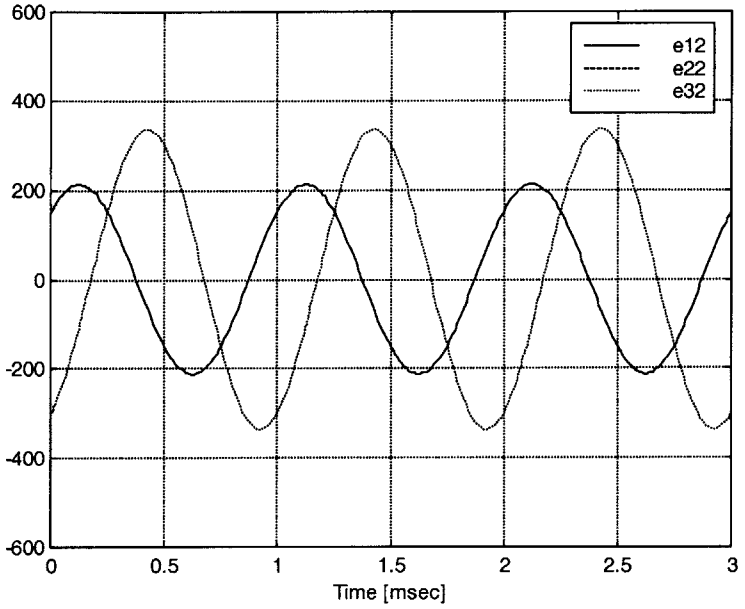

Figure 15: Voltage inputs for the second actuation system to achieve a linear motion.

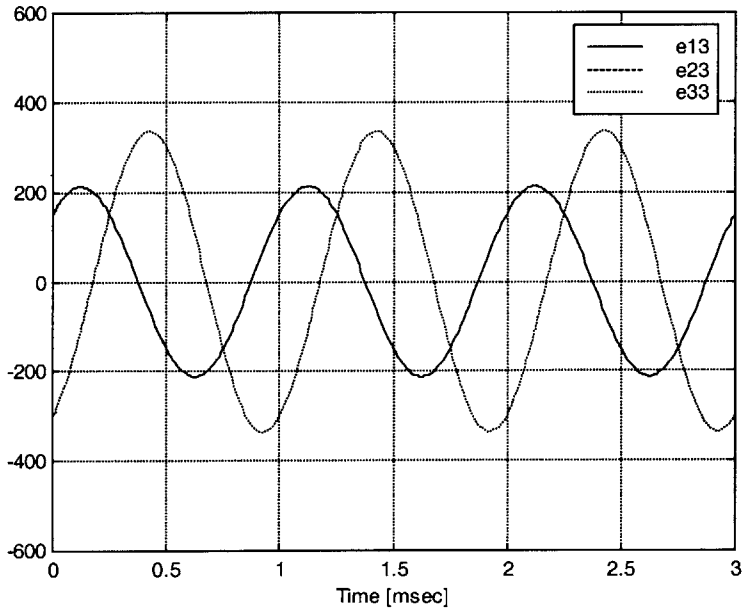

Figure 16: Voltage inputs for the third actuation system to achieve a linear motion.

4.3. Simulation of a rotational motion

In order to show a rotational motion of the stage, θ_1, θ_2, and θ_3 are chosen as 90, 210, and 330 degrees, respectively in this simulation as shown in Figure 17. Similarly, Figures 18-20 show the time responses of the stage motion. As expected, x and y components of the stage velocity are always zeros. The angular velocity of the stage is increased during the contact period, and this is decreased during the non-contact period. The x-y plot is separately shown in Figure 21. In this Figure, the x and y displacements are always zeros during the pure rotational motion as expected. For reference, Figures 22-24 show voltage input signals to each piezoelectric element of each actuation system.

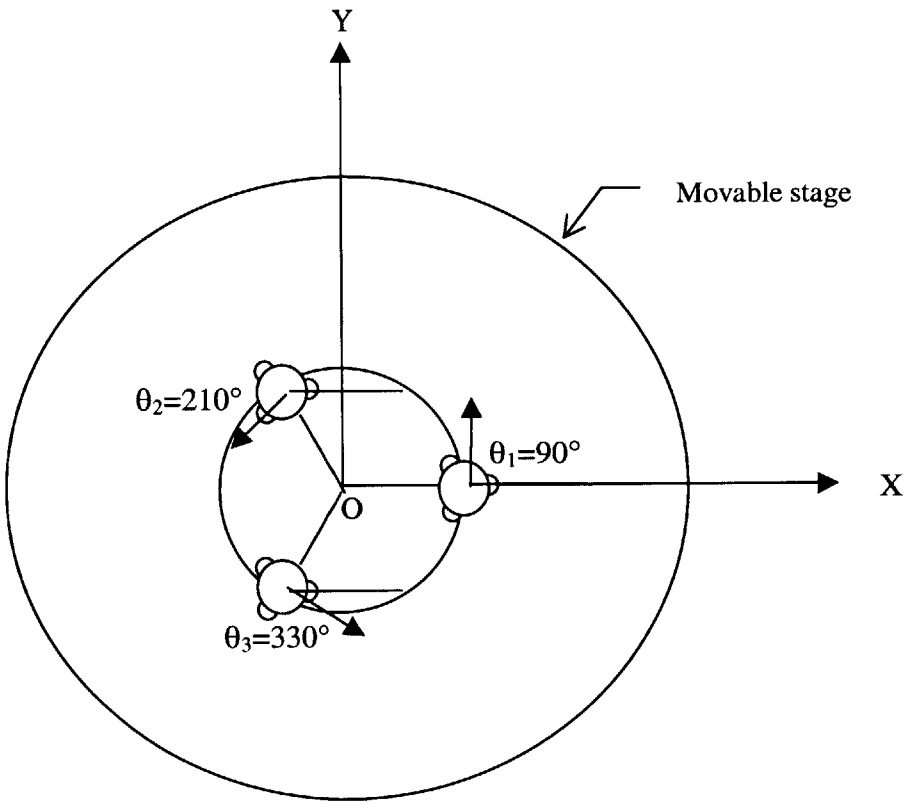

Figure 17: Schematic view of a 3 DOF friction drive stage rotating about Z.

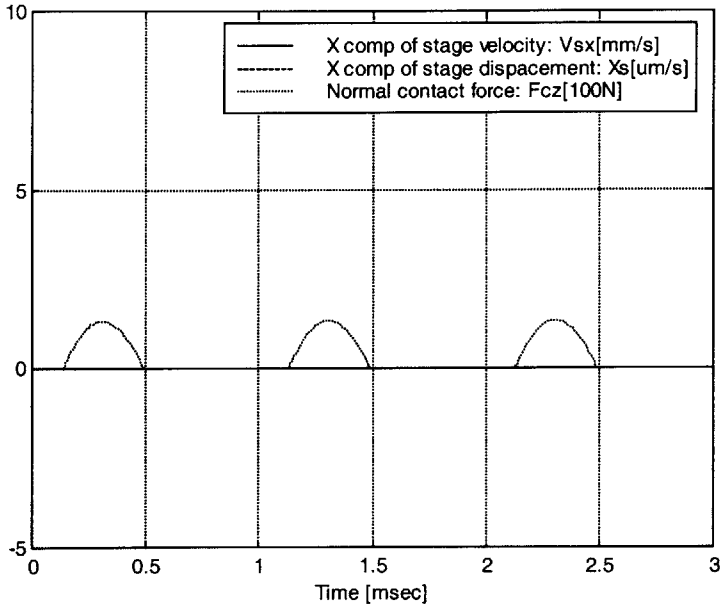

Figure 18: Time response of x component of stage velocity and displacement to achieve a rotational motion.

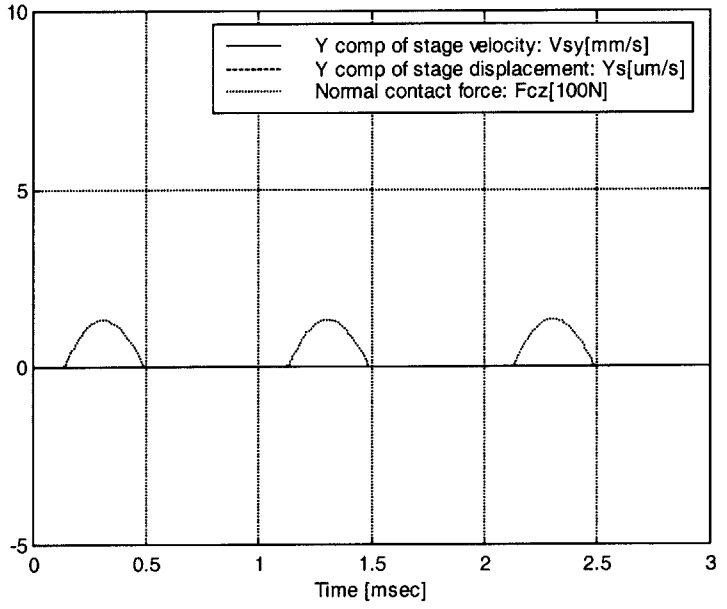

Figure 19: Time response of y component of stage velocity and displacement to achieve a rotational motion.

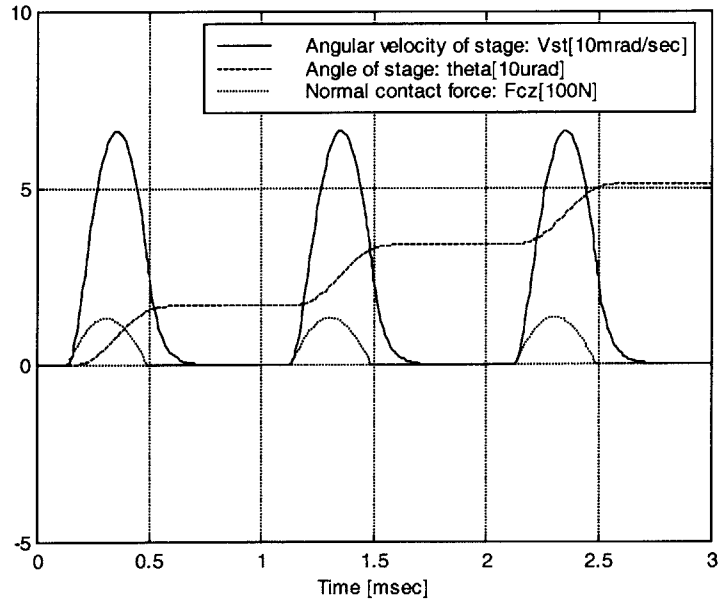

Figure 20: Time response of angular velocity and angle of the stage to achieve a rotational motion.

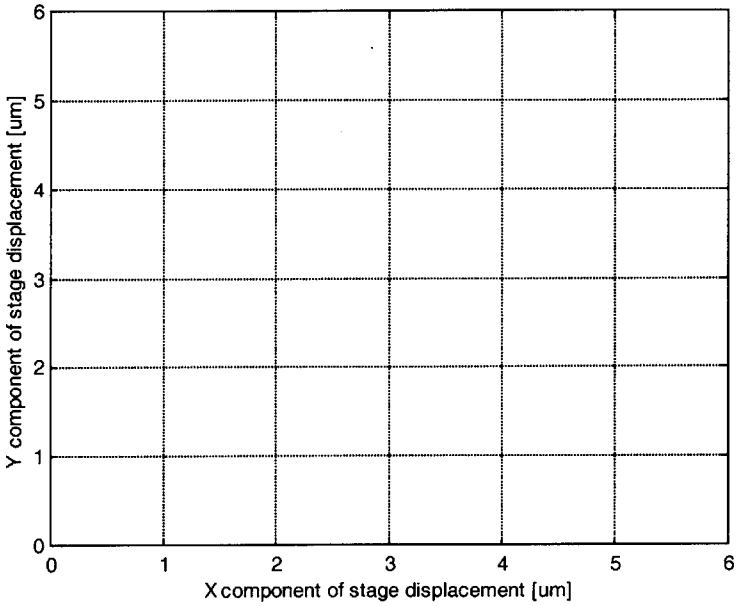

Figure 21: Trajectory of stage motion in XY plane to achieve a rotational motion. (The x and y displacements are always zeros during the pure rotational motion as expected.)

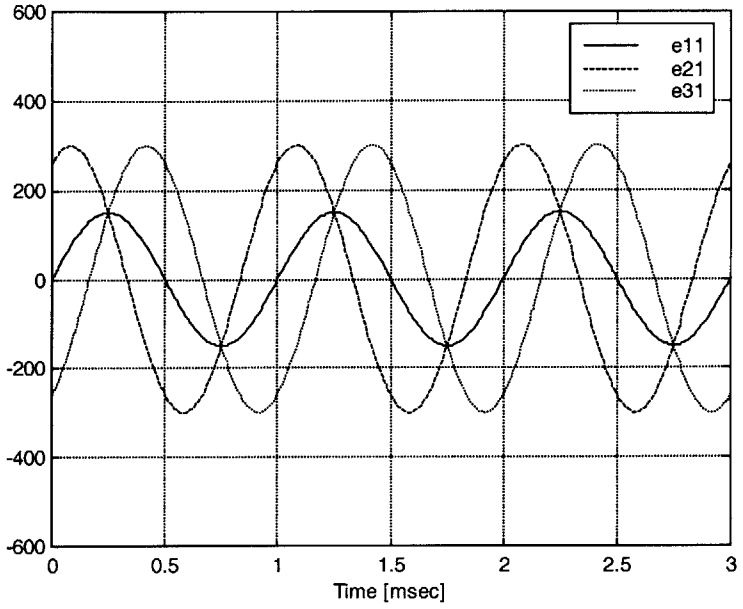

Figure 22: Voltage inputs for the first actuation system to achieve a rotational motion.

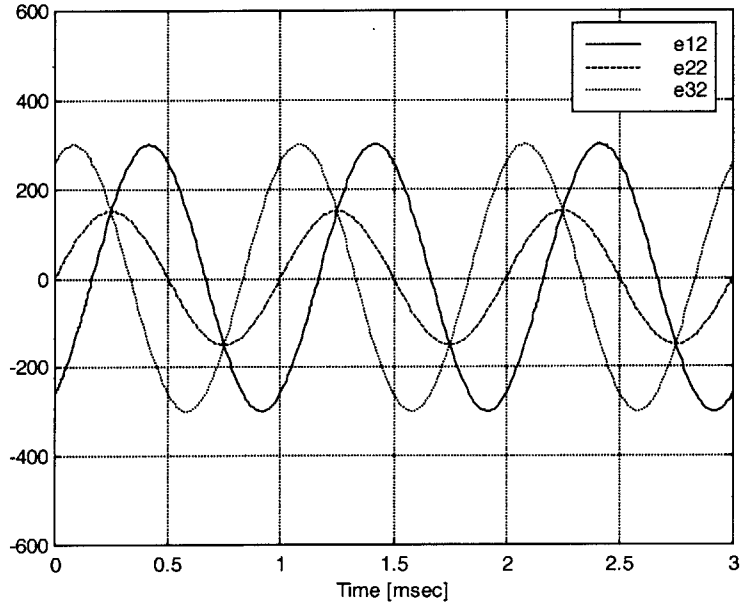

Figure 23: Voltage inputs for the second actuation system to achieve a rotational motion.

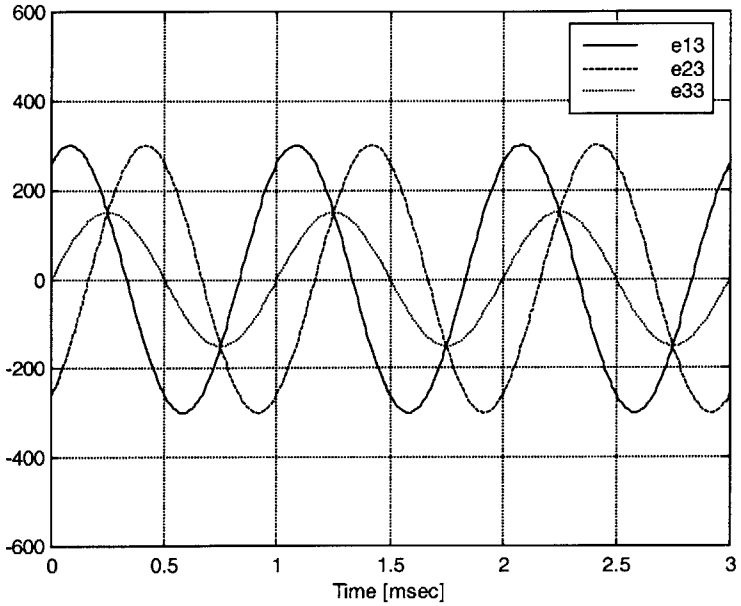

Figure 24: Voltage inputs for the third actuation system to achieve a rotational motion.

4.4. Simulation of a 3 DOF (linear plus rotational) motion

In order to show a linear plus rotational motion of the stage, θ_1, θ_2, θ_3 are chosen as 75, 135, 15 degrees, respectively in this simulation as shown in Figure 25. Similarly, Figures 26-28 show the time responses of the stage motion. As expected, x and y components of the stage velocity and angular velocity have non-zero but some values. The corresponding x-y plot is separately shown in Figure 29. Again, voltage input signals used in this simulation are shown in Figures 30-32.

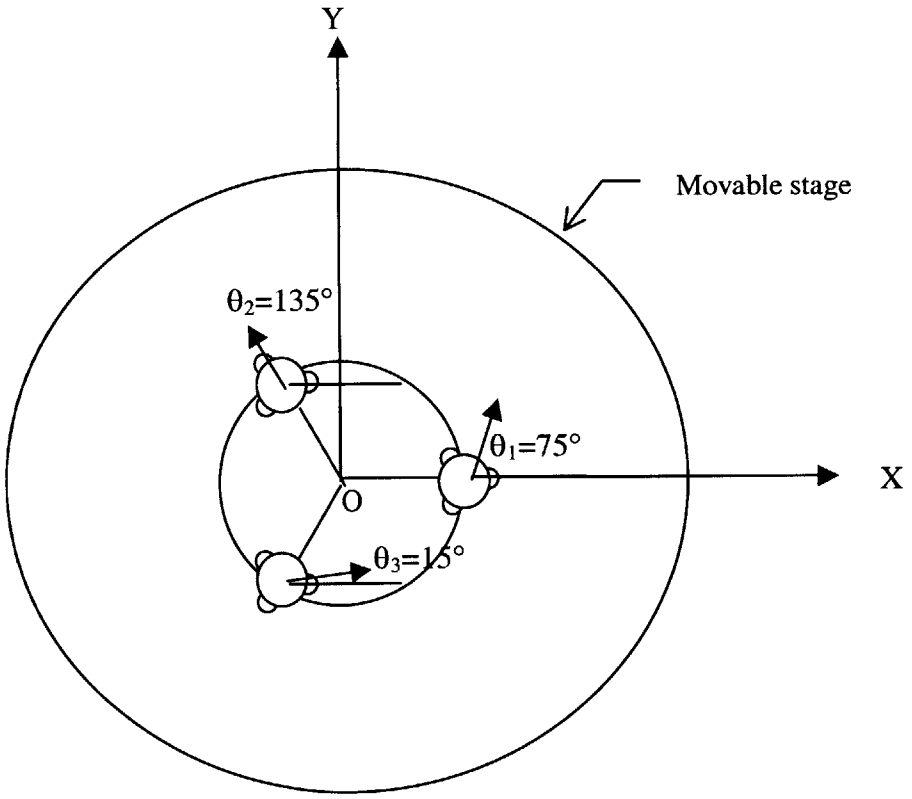

Figure 25: Schematic view of a 3 DOF friction drive stage moving linearly and rotating in XY plane.

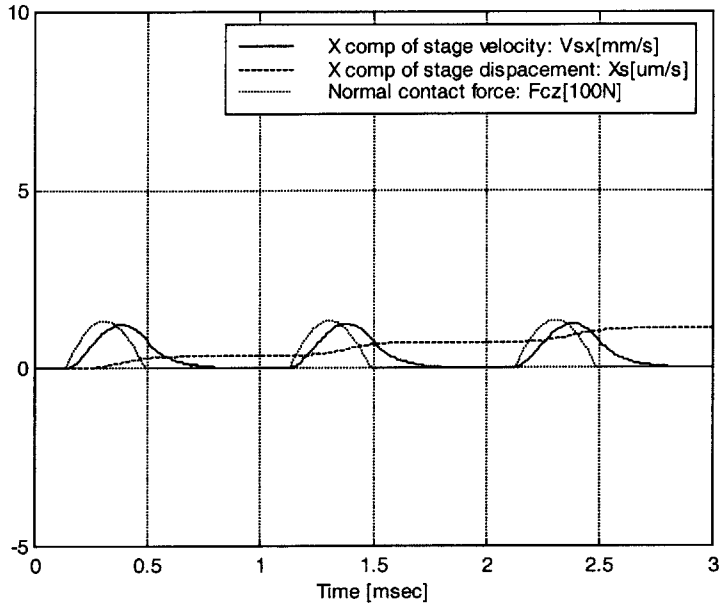

Figure 26: Time response of x component of stage velocity and displacement to achieve a linear plus rotational motion.

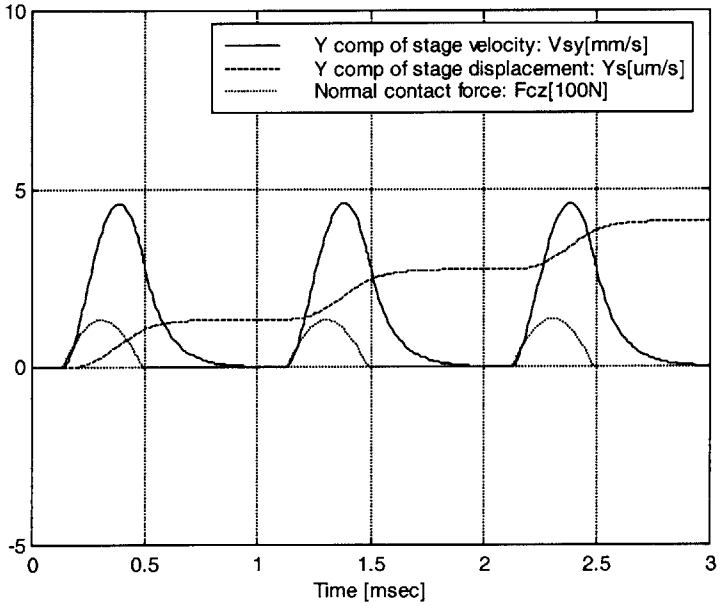

Figure 27: Time response of y component of stage velocity and displacement to achieve a linear plus rotational motion.

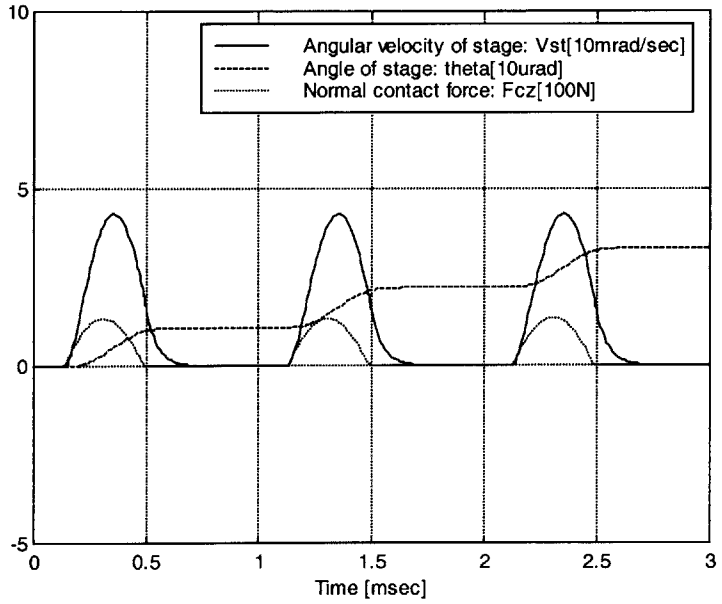

Figure 28: Time response of angular velocity and angle of the stage to achieve linear plus rotational motion.

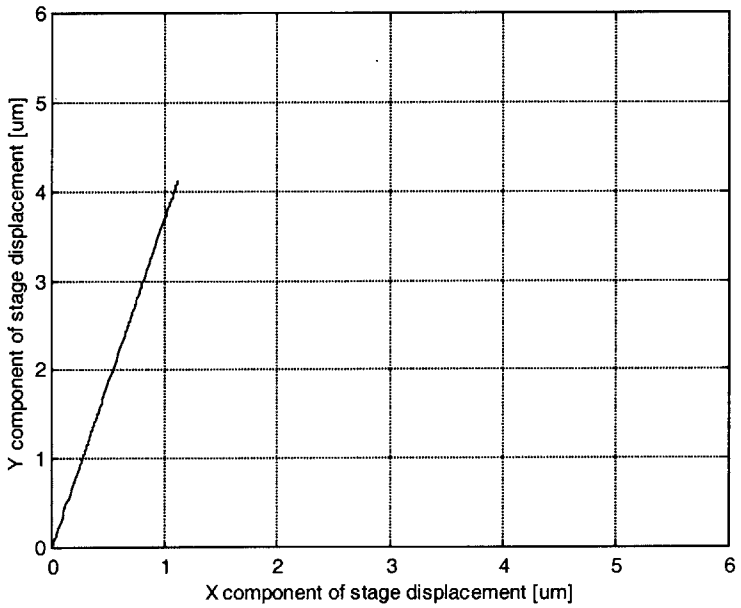

Figure 29: Trajectory of stage motion in XY plane to achieve a linear plus rotational motion.

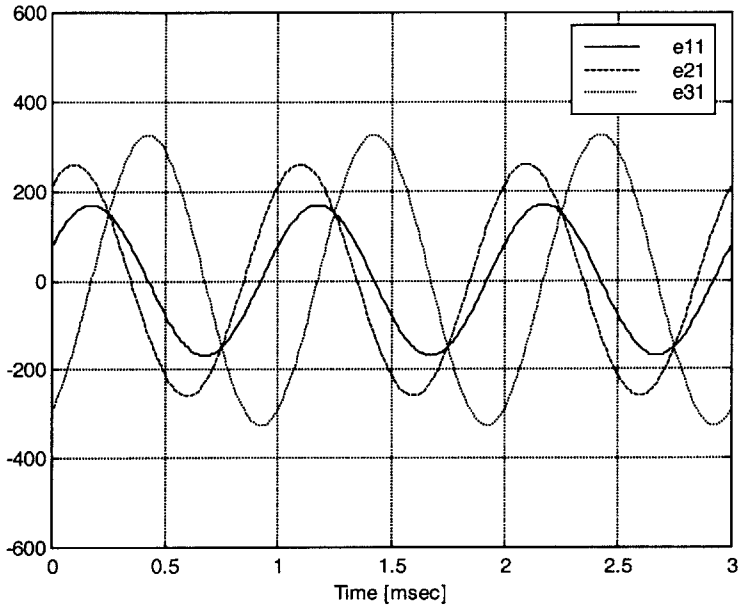

Figure 30: Voltage inputs for the first actuation system to achieve a linear plus rotational motion.

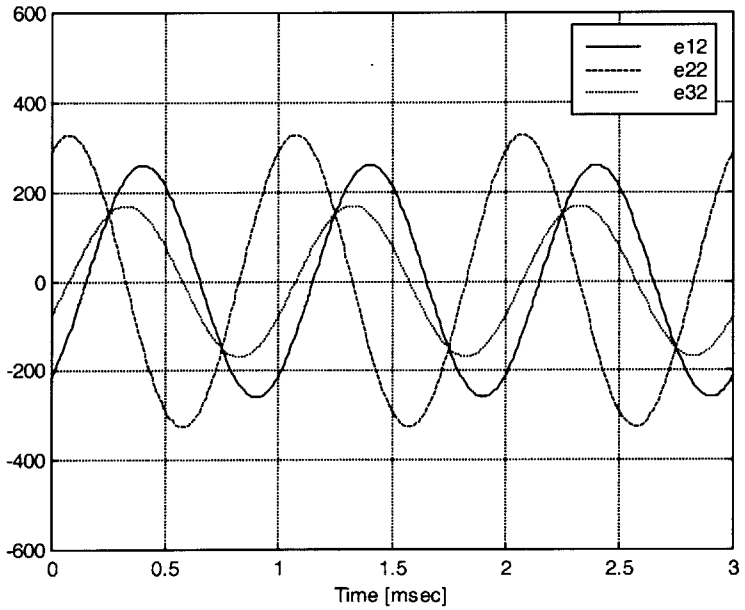

Figure 31: Voltage inputs for the second actuation system to achieve a linear plus rotational motion.

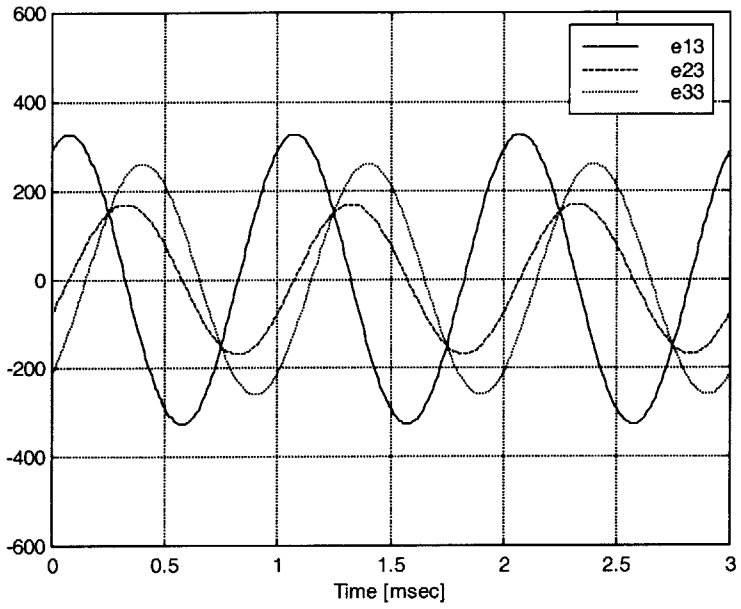

Figure 32: Voltage inputs for the third actuation system to achieve a linear plus rotational motion.

4.5. Summary

In this chapter, 3 DOF motion simulation was performed for the proposed friction drive stage system. It was shown that the proposed system could move linearly and/or rotationally as expected with proper voltage inputs.

5. Conclusion

A three degrees of freedom (DOF) positioning stage was proposed. The 3 DOF includes two linear (X and Y) and one rotational (θ) about Z. The proposed stage has advantages of simple structure as well as high precision positioning capability. For the 3 DOF motion, the stage needs one movable stage and three directional actuation systems. For a proposed directional actuation system, the kinematic analysis was performed. For the proposed stage system with one movable stage and three directional actuation systems, dynamic modeling was done. This modeling led to a clear understanding of the stage motion using a friction drive. In addition, the controllability and observability of 3 DOF stage was presented. Simulation results for the dynamic model showed that the 3 DOF motion of the proposed stage worked as expected. It is believed that the proposed stage can be a good candidate for high precision 3 DOF positioning stage systems.

Bibliography

[Adachi] K. Adachi and K. Kato, "Transmission Systems of Motion and Force - Friction Drive/Traction Drive," Journal of Japan Society of Precision Engineers, Vol. 60, No. 10, pp. 1410-1415, 1994.

[Burleigh] "The Micropositioning Book, Burleigh Instruments, Inc.", Burleigh Park, Fishers, NY, 14453, 1990.

[Cai92] H. Cai, L. Sun and Y. Zhang, "A New Force-Controlled Micro Robotic Worktable Driven by Piezoelectric Elements," Proceedings of the IMAC/SICE International Symposium on Robotics, Mechatronics and Manufacturing Systems, pp. 637-642, 1992.

[Ferreira95] A. Ferreira, P. Minotti and P. Le Moal, "New Multi-Degree of Freedom Piezoelectric Micromotors for Micromanupulator Applications," Proceedings of IEEE Ultrasonic Symposium, pp. 417-422, 1995.

[Hoshi95] N. Hoshi and A. Kawamura, "Analysis of Plane Ultrasonic Piezoelectric Actuators," IEEE Industry Applications Magazine, July/August, pp. 23-29, 1995.

[Kurosawa96] M. Kurosawa, M. Takahashi, T. Higuchi, "Ultrasonic Linear Motor Using Surface Acoustic Wave," IEEE Trans. on Ultrasonics, Ferroelectrics, and Frequency Control (UFFC), Vol. 43, No. 5, pp. 901-906, 1996.

[Mori89] K. Mori, T. Kumagae and H. Hirai, "Ultrasonic Linear Motor for a High Precision X-Y Stage," Proceedings of IEEE Ultrasonic Symposium, pp. 657-660, 1989.

[Nikkei] Nikkei Mechanical, No. 507, pp. 74-79, May 26, 1997 (in Japanese).

[Ohara96] T. Ohara, "A New High Precision Position Measurement System," MIT Ph.D. dissertation, p.3, 1996.

[Ro94] P. I. Ro et al., "Nanometric Motion Control of a Traction Drive," DSC-Vol. 55-2, Dynamic Systems and Control: Vol.2 ASME, pp. 879-883, 1994.

[Sakuta96] S. Sakuta, et al., "Precision Table Control System by Friction Drive for Optical Disk Mastering Machine," Journal or Japan Society of Precision Engineers, Vol. 62, No. 10, pp. 1444-1448, 1996.

[Choi96] H. Choi, "A Linear Ultrasonic Motor for Nano-Technology", Master's Thesis, 1996, MIT.

[Ueha93] S. Ueha and Y. Tomikawa, "Ultrasonic Motors Theory and Applications," Oxford Science Publications, 1993.

Appendix: Matlab simulation codes

```
% file name: s77.m
% 5/6/1999
% main motion simulation program for 3DOF friction drive stage motion

global freq omega theta_d1 theta_d2 theta_d3 ms I ma cm N g fp kz0 bs bi ba
global myu delta r ra rp v01 v02 v03 vr
global j11 j12 j13 j21 j22 j23 j31 j32 j33 bx by bz
global a1 b1 a2 b2 a3 b3
global e11 e21 e31 e12 e22 e32 e13 e23 e33


%simulation parameters
direction1=75;
direction2=135;
direction3=15;
freq=10^3;
v01=150;
v02=150;
v03=150;
t0=0; tf=3*1/freq;
%end of simulation parameters

%linear motion example: direction1=60;direction2=60;direction3=60
%rotational motion example: direction1=90;direction2=210;direction3=330
%linear plus rotational motion example: direction1=75;direction2=135;direction3=15

theta_d1=pi/180*direction1;
theta_d2=pi/180*direction2;
theta_d3=pi/180*direction3;

ms=1;
I=1/2*(0.1)^2;
ma=0.1;
cm=0.02*10^(-6);
N=8;
g=9.81;
fp=100;

bs=10000;
bi=100;
kz0=10^(7);
bx=10;
myu=0.2;

by=bx;
ba=3000;
bz=10000;

delta=10*10^(-6);
r=2*10^(-2);
ra=8*10^(-2);
rp=2*10^(-2);

%vr=x_0/z_0
vr=2;

%positions of three actuation systems
a1=ra*cos(0);      b1=ra*sin(0);
a2=ra*cos(2*pi/3); b2=ra*sin(2*pi/3);
a3=ra*cos(4*pi/3); b3=ra*sin(4*pi/3);

%positions of three piezoelectric elements
x1=r*cos(0);      y1=r*sin(0);
x2=r*cos(2*pi/3); y2=r*sin(2*pi/3);
x3=r*cos(4*pi/3); y3=r*sin(4*pi/3);
det=(x2*y3-x3*y2)-(x1*y3-x3*y1)+(x1*y2-x2*y1);
```

```
%calculation of Jacobian matrix
j11=rp*(y3-y2)/det; j12=rp*(y1-y3)/det; j13=rp*(y2-y1)/det;
j21=rp*(x2-x3)/det; j22=rp*(x3-x1)/det; j23=rp*(x1-x2)/det;
j31=1/3          ; j32=1/3          ; j33=1/3          ;

%initial conditions
x0=[0 0 0 0 0 0 0 0 0 0 0 0 0 0 0 0 0 0 0 0 0 0 0 0 0 0 0 0 0 0 0 0 0 0 0 0];
[t,x]=ode45('d77',[t0 tf],x0);

%x(1)=x velocity of stage, x(2)=y velocity of stage, x(3)=theta velocity of stage
%x(34)=x displacement of stage, x(35)=y displacement of stage, x(36)=theta displacement of stage
%x(4)=normal contact force


figure
plot(t*10^3,x(:,1)*10^3,'k-',t*10^3,x(:,34)*10^6,'k--',t*10^3,x(:,4)/100,'k:')
legend('X comp of stage velocity: Vsx[mm/s]',...
       'X comp of stage dispacement: Xs[um/s]',...
       'Normal contact force: Fcz[100N]')
axis([0,3,-5,10])
grid
xlabel('Time [msec]')
%ylabel('Xs[um],Ys[um],Theta[10mrad],Vsx[mm/s],Vsy[mm/s],Fcz[kN]')
%title('Time response of 3 DOF stage motion')

figure
plot(t*10^3,x(:,2)*10^3,'k-',t*10^3,x(:,35)*10^6,'k--',t*10^3,x(:,4)/100,'k:')
legend('Y comp of stage velocity: Vsy[mm/s]',...
       'Y comp of stage displacement: Ys[um/s]',...
       'Normal contact force: Fcz[100N]')
axis([0,3,-5,10])
grid
xlabel('Time [msec]')

figure
plot(t*10^3,x(:,3)*10^2,'k-',t*10^3,x(:,36)*10^5,'k--',t*10^3,x(:,4)/100,'k:')
legend('Angular velocity of stage: Vst[10mrad/sec]',...
       'Angle of stage: theta[10urad]',...
       'Normal contact force: Fcz[100N]')
axis([0,3,-5,10])
grid
xlabel('Time [msec]')

figure
plot(t*10^3,(v01*sin(omega*t)+cos(theta_d1)*vr*v01*cos(omega*t)*r/rp),'k-',...
     t*10^3,(v01*sin(omega*t)-cos(pi/3+theta_d1)*vr*v01*cos(omega*t)*r/rp),'k--',...
     t*10^3,(v01*sin(omega*t)-cos(pi/3-theta_d1)*vr*v01*cos(omega*t)*r/rp),'k:')
     legend('e11', 'e21', 'e31')
axis([0,3,-600,600])
grid
xlabel('Time [msec]')

figure
plot(t*10^3,(v02*sin(omega*t)+cos(theta_d2)*vr*v02*cos(omega*t)*r/rp),'k-',...
     t*10^3,(v02*sin(omega*t)-cos(pi/3+theta_d2)*vr*v02*cos(omega*t)*r/rp),'k--',...
     t*10^3,(v02*sin(omega*t)-cos(pi/3-theta_d2)*vr*v02*cos(omega*t)*r/rp),'k:')
     legend('e12', 'e22', 'e32')
axis([0,3,-600,600])
grid
xlabel('Time [msec]')

figure
plot(t*10^3,(v03*sin(omega*t)+cos(theta_d3)*vr*v03*cos(omega*t)*r/rp),'k-',...
     t*10^3,(v03*sin(omega*t)-cos(pi/3+theta_d3)*vr*v03*cos(omega*t)*r/rp),'k--',...
     t*10^3,(v03*sin(omega*t)-cos(pi/3-theta_d3)*vr*v03*cos(omega*t)*r/rp),'k:')
legend('e13', 'e23', 'e33')
axis([0,3,-600,600])
grid
xlabel('Time [msec]')

figure
```

```
plot(x(:,34)*1e6,x(:,35)*1e6,'k-')
axis ([0, 6, 0, 6])
grid
xlabel('X component of stage displacement [um]')
ylabel('Y component of stage displacement [um]')
```

```
% file name: d77.m
% 5/6/1999
% differential equation for the 3 DOF motion simulation (s77) of the stage

function xdot=d77(t,x)

global freq omega theta_d1 theta_d2 theta_d3 ms I ma cm N g fp kz0 bs bi ba
global myu delta r ra rp v01 v02 v03 vr
global j11 j12 j13 j21 j22 j23 j31 j32 j33 bx by bz
global a1 b1 a2 b2 a3 b3
global e11 e21 e31 e12 e22 e32 e13 e23 e33

omega=2*pi*freq;

%control voltage inputs to 9 piezoelectric elements
%eij represents voltage input to the i_th element of the j_th actuation system
e11=v01*sin(omega*t)+cos(theta_d1)*vr*v01*cos(omega*t)*r/rp;
e21=v01*sin(omega*t)-cos(pi/3+theta_d1)*vr*v01*cos(omega*t)*r/rp;
e31=v01*sin(omega*t)-cos(pi/3-theta_d1)*vr*v01*cos(omega*t)*r/rp;
e12=v02*sin(omega*t)+cos(theta_d2)*vr*v02*cos(omega*t)*r/rp;
e22=v02*sin(omega*t)-cos(pi/3+theta_d2)*vr*v02*cos(omega*t)*r/rp;
e32=v02*sin(omega*t)-cos(pi/3-theta_d2)*vr*v02*cos(omega*t)*r/rp;
e13=v03*sin(omega*t)+cos(theta_d3)*vr*v03*cos(omega*t)*r/rp;
e23=v03*sin(omega*t)-cos(pi/3+theta_d3)*vr*v03*cos(omega*t)*r/rp;
e33=v03*sin(omega*t)-cos(pi/3-theta_d3)*vr*v03*cos(omega*t)*r/rp;

%vaij represents the i component of the tip velocity of the j_th actuation system
vax1=j11*x(7)+j12*x(8)+j13*x(9);
vay1=j21*x(7)+j22*x(8)+j23*x(9);
vaz1=j31*x(7)+j32*x(8)+j33*x(9);
vax2=j11*x(10)+j12*x(11)+j13*x(12);
vay2=j21*x(10)+j22*x(11)+j23*x(12);
vaz2=j31*x(10)+j32*x(11)+j33*x(12);
vax3=j11*x(13)+j12*x(14)+j13*x(15);
vay3=j21*x(13)+j22*x(14)+j23*x(15);
vaz3=j31*x(13)+j32*x(14)+j33*x(15);
za1=j31*x(25)+j32*x(26)+j33*x(27);
za2=j31*x(28)+j32*x(29)+j33*x(30);
za3=j31*x(31)+j32*x(32)+j33*x(33);

%contact and non-contact condition
if (za1>=delta)
   fz1=x(4);
   del_vx1=vax1-(x(1)-b1*x(3));
   del_vy1=vay1-(x(2)+a1*x(3));
   vabs1=sqrt(del_vx1^2+del_vy1^2);
   fx1=myu*sign(del_vx1)*fz1*abs(del_vx1)/vabs1+bx*(del_vx1);
   fy1=myu*sign(del_vy1)*fz1*abs(del_vy1)/vabs1+by*(del_vy1);
   F11=j11*fx1+j21*fy1+j31*fz1;
   F21=j12*fx1+j22*fy1+j32*fz1;
   F31=j13*fx1+j23*fy1+j33*fz1;
   kz1=kz0;
else
   kz1=0;
   fx1=0;fy1=0;fz1=0;
   F11=0;F21=0;F31=0;
end

if (za2>=delta)
   fz2=x(5);
   del_vx2=vax2-(x(1)-b2*x(3));
   del_vy2=vay2-(x(2)+a2*x(3));
   vabs2=sqrt(del_vx2^2+del_vy2^2);
   fx2=myu*sign(del_vx2)*fz2*abs(del_vx2)/vabs2+bx*(del_vx2);
   fy2=myu*sign(del_vy2)*fz2*abs(del_vy2)/vabs2+by*(del_vy2);
   F12=j11*fx2+j21*fy2+j31*fz2;
   F22=j12*fx2+j22*fy2+j32*fz2;
   F32=j13*fx2+j23*fy2+j33*fz2;
   kz2=kz0;
else
   kz2=0;
```

```
    fx2=0;fy2=0;fz2=0;
    F12=0;F22=0;F32=0;
end

if (za3>=delta)
    fz3=x(6);
    del_vx3=vax3-(x(1)-b3*x(3));
    del_vy3=vay3-(x(2)+a3*x(3));
    vabs3=sqrt(del_vx3^2+del_vy3^2);
    fx3=myu*sign(del_vx3)*fz3*abs(del_vx3)/vabs3+bx*(del_vx3);
    fy3=myu*sign(del_vy3)*fz3*abs(del_vy3)/vabs3+by*(del_vy3);
    F13=j11*fx3+j21*fy3+j31*fz3;
    F23=j12*fx3+j22*fy3+j32*fz3;
    F33=j13*fx3+j23*fy3+j33*fz3;
    kz3=kz0;
else
    kz3=0;
    fx3=0;fy3=0;fz3=0;
    F13=0;F23=0;F33=0;
end
%end of contact and non-contact condition

%state equations
    xdot(1)=-(bs/ms*x(1))+1/ms*(fx1+fx2+fx3);
    xdot(2)=-(bs/ms*x(2))+1/ms*(fy1+fy2+fy3);
    xdot(3)=-(bi/I*x(3))+1/I*(-x(34)*(fy1+fy2+fy3)+x(35)*(fx1+fx2+fx3)...
            +a1*fy1+a2*fy2+a3*fy3-(b1*fx1+b2*fx2+b3*fx3));
    xdot(4)=kz1*vaz1;
    xdot(5)=kz2*vaz2;
    xdot(6)=kz3*vaz3;
    xdot(7)=-1/ma*x(16)-ba/ma*x(7)-F11/ma+1/ma*N*e11;
    xdot(8)=-1/ma*x(17)-ba/ma*x(8)-F21/ma+1/ma*N*e21;
    xdot(9)=-1/ma*x(18)-ba/ma*x(9)-F31/ma+1/ma*N*e31;
    xdot(10)=-1/ma*x(19)-ba/ma*x(10)-F12/ma+1/ma*N*e12;
    xdot(11)=-1/ma*x(20)-ba/ma*x(11)-F22/ma+1/ma*N*e22;
    xdot(12)=-1/ma*x(21)-ba/ma*x(12)-F32/ma+1/ma*N*e32;
    xdot(13)=-1/ma*x(22)-ba/ma*x(13)-F13/ma+1/ma*N*e13;
    xdot(14)=-1/ma*x(23)-ba/ma*x(14)-F23/ma+1/ma*N*e23;
    xdot(15)=-1/ma*x(24)-ba/ma*x(15)-F33/ma+1/ma*N*e33;
    xdot(16)=1/cm*x(7);
    xdot(17)=1/cm*x(8);
    xdot(18)=1/cm*x(9);
    xdot(19)=1/cm*x(10);
    xdot(20)=1/cm*x(11);
    xdot(21)=1/cm*x(12);
    xdot(22)=1/cm*x(13);
    xdot(23)=1/cm*x(14);
    xdot(24)=1/cm*x(15);
    xdot(25)=x(7);
    xdot(26)=x(8);
    xdot(27)=x(9);
    xdot(28)=x(10);
    xdot(29)=x(11);
    xdot(30)=x(12);
    xdot(31)=x(13);
    xdot(32)=x(14);
    xdot(33)=x(15);
    xdot(34)=x(1);
    xdot(35)=x(2);
    xdot(36)=x(3);

xdot=xdot';
```